PB89-164560

HEGADAS: Heavy Gas Dispersion Program User's Guide

Shell Research Ltd., Chester (England)

Prepared for

Environmental Protection Agency
Research Triangle Park, NC

Aug 88

U.S. Department of Commerce
National Technical Information Service
NTIS

TECHNICAL REPORT DATA

(Please read Instructions on the reverse before completing)

1. REPORT NO. EPA/SW/DK-89/027a R-1681	2.
3. RECIPIENT'S ACCESSION NO. PB89-164560	
4. TITLE AND SUBTITLE HEGADAS* Heavy Gas Dispersion Program Users Guide * Shell Trademark	5. REPORT DATE January 1989 6. PERFORMING ORGANIZATION CODE
7. AUTHOR(S) J. S. Puttock, G. W. Colenbrander, and H. W. M. Witlox	8. PERFORMING ORGANIZATION REPORT NO
9. PERFORMING ORGANIZATION NAME AND ADDRESS Shell Research Ltd., Combustion Division Thornton Research Center P. O. Box 1 Chester, England CH1 3SH	10. PROGRAM ELEMENT NO. 11. CONTRACT/GRANT NO.
12. SPONSORING AGENCY NAME AND ADDRESS Environmental Protection Agency Office of Air Quality Planning and Standards Technical Support Division (MD-14) Research Triangle Park, NC 27711	13. TYPE OF REPORT AND PERIOD COVERED 14. SPONSORING AGENCY CODE
15. SUPPLEMENTARY NOTES For diskettes, see: PB89-164552	

16. ABSTRACT

The HEGADAS program models the dispersion of releases of heavier-than-air gases to the atmosphere. The model is an integral model which uses assumed profile (e.g., concentration profile) shapes and empirical relations describing air entrainment. The model provides for a smooth transition to passive dispersion. Descriptions of heat transfer from the ground and water vapor transfer are also included. The source release rate may be constant or time-dependent (e.g., evaporating liquid pool).

17. KEY WORDS AND DOCUMENT ANALYSIS

a. DESCRIPTORS	b. IDENTIFIERS/OPEN ENDED TERMS	c. COSATI Field/Group
- Mathematical Model - Air pollution - Dispersion - Computer program	- HEGADAS - Dense Gas Dispersion Modeling	

18. DISTRIBUTION STATEMENT Unlimited	19. SECURITY CLASS *(This Report)*	21. NO. OF PAGES 185
	20. SECURITY CLASS *(This page)*	22. PRICE A06

EPA Form 2220-1 (Rev. 4-77) PREVIOUS EDITION IS OBSOLETE

PB89-164560

USER'S GUIDE FOR THE

HEGADAS*

HEAVY GAS DISPERSION PROGRAM

by

H.W.M. Witlox

Copyright, 1988
Shell Oil Company
All Rights Reserved

August 1988

Shell Research Ltd.
Combustion Division
Thornton Research Center
P. O. Box 1
Chester, England CH1 3SH

* Shell Trademark

REPRODUCED BY
U.S. DEPARTMENT OF COMMERCE
NATIONAL TECHNICAL INFORMATION SERVICE
SPRINGFIELD, VA. 22161

The user may copy and distribute the HEGADAS program or include the HEGADAS program, in whole or in part, in another computer program provided that the following conditions are met:

1. No fee may be charged for copying or distributing the HEGADAS program or any part thereof without the written permission of Shell Oil Company

2. The HEGADAS program may not be distributed, in whole or in part, as part of any commercial product without the written permission of Shell Oil Company.

This computer program is provided "as is" and on the condition that:

No warranty express or implied is given regarding the content or use of the computer program, the data upon which the same is based, or the results to be obtained from the use thereof; or given as to merchantability or fitness for a particular purpose; or that the use of this program will not infringe any patent.

CONTENTS

1. Introduction 2

2. Installation of the HEGADAS program 3

3. The HEGADAS input data file 5

4. The HEGADAS run 7

5. The HEGADAS output data file 9

References 10

Appendix A. Listing of HEGADAS input data files (examples) 11

Tables 14

Figure 22

Appendix B. Dispersion of Releases of Dense Gas:
Development of the HEGADAS Model

1. INTRODUCTION

In this report a user's guide to the steady-state and transient versions of the HEGADAS heavy-gas-dispersion program is provided. The technical description of the dispersion model which forms the basis of HEGADAS program is contained in references 1 and 2. This guide makes frequent cross-references to these references; in the data-input tables references of the form 2(5.1), for example, refer to section 5.1 of reference 2.

This document is to be provided with the public release of the PC-version of the HEGADAS program. In Section 2 the installation of this version is described, and the constituent files are given. Section 3 describes the layout of the free-format HEGADAS input data file, Section 4 the performance of a HEGADAS run, and Section 5 the layout of the HEGADAS output data file.

2. INSTALLATION OF PC-VERSION OF THE HEGADAS PROGRAM

Hardware

The HEGADAS program requires 512K memory, a math coprocessor and PCDOS/MSDOS version 3.1 or higher. The program has been tested on an IBM AT (80286/7), an IBM XT (8088/7), and an IBM PS2 Model 50 (80286/7). The program requires that the environment space be increased to 1024 bytes over the DOS default of 128 bytes. Programs that are resident on your PC may claim environment space and therefore should not be loaded when running the HEGADAS programs. Similarly, commands such as SET and PATH reserve environment space and their use should be minimised.

To increase allocation of environment space include, exactly as it appears, the following command in the file CONFIG.SYS:

```
shell=c:\command.com /e:1024 c:\ /p
```

Software

The HEGADAS program involves the following files.

1. Files associated with the HEGADAS data dictionaries, which define the input panels, the panel keywords, and their allowable ranges; see Section 3 for further details. The user may modify the data in the HEGADAS dictionaries by the following two consecutive steps.

- Implementation of the modification by editing the dictionary-definition files HGSDDF.DCT (steady-state) or HGTDDF.DCT (transient).
- Execution of the batch files HGSDD.BAT (steady-state; simply type "HGSDD") or HGTDD (transient; type "HGTDD"). These batch files generate the new "machine-code" data-dictionary files DICT.HSD and DICT.HTD by calling the program DDMAIN.EXE.

2. Program FFMAIN.EXE which validates the free-format HEGADAS input data file, and the programs HSMAIN.EXE (steady-state) and HTMAIN.EXE (transient), which perform the actual HEGADAS calculations. These programs are called via the batch files HEGADASS.BAT and HEGADAST.BAT, respectively; see Section 4 for further details.

3. Source files (.FOR files) associated with the above executables DDMAIN.EXE, FFMAIN.EXE, HSMAIN.EXE and HTMAIN.EXE, and corresponding "include" files (common blocks; .INC files).

4. HEGADAS input data files (.HSI and .HTI files; see Section 3) and output data files (.HSR and .HTR files; see Section 5). With the public HEGADAS release two example input data files, TEST.HSI (steady-state) and TEST.HTI (transient state) are provided; see Appendix A for a listing of these files.

5. Temporary files which are generated during a HEGADAS run, but which are deleted at the end of the run.

3. THE HEGADAS INPUT DATA FILE

The user needs to specify the characteristics of the dense-gas dispersion problem in the free-format HEGADAS input data file. This file must have an extension .HSI for a steady-state run or .HTI for a time-dependent run. It is easiest to generate an input file by copying and editing an existing file because the layout and comments, described below, assist data entry. See Appendix A for examples of input data files.

The information in the input file is divided into groups of like parameters and each group, or panel, has an identifying keyword or keyphrase. Within each panel individual parameter values are assigned to named variables which are themselves keywords. The HEGADAS program uses these variable keywords to retrieve data from the input file. As shown in the following example for the panel "AMBIENT CONDITIONS", each parameter value is followed by an asterisk which marks the start of a comment giving the units used and the parameter's role.

```
*
AMBIENT CONDITIONS
*

  AIRTEMP  =  0.14E+2     *    C          AIR TEMP. AT GROUND LEVEL
  RH       =  0.90        *               RELATIVE HUMIDITY
  UO       =  0.30E+1     *    M/S        WIND VELOCITY AT HEIGHT ZO
  ZO       =  0.10E+2     *    M          REFERENCE HEIGHT
  TGROUND  =  0.14E+2     *    C          EARTH-S SURFACE TEMPERATURE

*
```

Tables Ia and Ib include a description of all panels and constituent input parameters for the steady-state and transient runs, respectively. The following should be noted:

- The keyword for each panel is indicated. Note that in the "TITLE" and "SKIP" panels, together with the optional "DISTS" panel, the panel keyword is itself followed by data.

- For each variable, the (current) allowed range for the input data, comprising minimum and maximum values, is given (defined in the data dictionaries). For a further description of the input parameters reference is made to reference 1 or sections in reference 2.

- Except for the "TSTAR" and "SOURCE" variables, all keywords should not occur more than once.

- The presence of the "DISTS" panel is optional. This panel allows the HEGADAS calculations to be interrupted at a specified break-point, x_s, downwind of the source and then restarted with user-specified values for several variables which are passed through the "DISTS" panel.

4. THE HEGADAS RUN

To run the steady state HEGADAS program, change the currently selected directory to the appropriate subdirectory (e.g. CD \HEGADASS), and then type HEGADASS followed by the input data filename, omitting the .HSI extension (e.g. HEGADASS TESTA). For the time dependent version the procedure is the same with the name HEGADAST replacing HEGADASS.

A HEGADAS run consists of the following consecutive steps. (Note that steps III and IV are performed for each timestep in a transient run).

I. Data validation

- The values of the input data are checked. If one or more of these values is out of range, appropriate error messages are inserted into the input data file and the program terminates. When the data values have been corrected these error messages will be deleted automatically.

II. Matching of wind profile

- The exponent α and ambient friction velocity u_* are determined by matching the similarity wind profile with the conventional logarithmic wind profile.

III. Source description

- At low source strengths a gas blanket may not be formed. In this case the source dimensions are taken to be that of the primary source. The concentration along the source is found in an iterative manner; see Section 4.2 in Reference 2.

- If a 100% gas blanket forms then the dimensions L, B of the secondary source are larger than the dimensions L_p, B_p of the primary source and must be calculated. The source length L is then found in an iterative manner (see Ref. 2.) and the source breadth is scaled according to $B = B_p L/L_p$.

- Note that along the source the concentration is assumed to be constant and that there is no horizontal spreading ($b=B$, $S_y=0$). The dispersion coefficient S_z is found by numerical integration of eq. (E.12) in Reference 2.

IV. Solution downwind of the source

The governing equations (see Appendix E of reference 2) are integrated until a threshold concentration, specified as input data, is reached. The calculations can include surface heat transfer and also water vapour pickup or neglect both according to the value set for the variable "ISURF" in the "TITLE" panel. The (maximum) calculation step-length, which is also the reporting interval for the output data, is specified as a fraction of the source length L in the input data. Because the source length L depends on other input conditions the calculation step length can vary between runs.

5. THE HEGADAS OUTPUT DATA FILE

The output file has the same name as the input file and an extension of .HSR for the steady state run, .HTR for the time dependent case. The output generated during a HEGADAS run comprises:

I. A copy of the values of the input parameters, which are specified in the HEGADAS input file.

II. The values of the calculated wind profile parameters

III. The dimensions of the secondary source and the take-up flux for the secondary source.

IV. Output data for points downwind of the source.

Table II includes a description of the output data produced in steps III and IV and more details are given in reference 2.

The cumulative cloud data are produced for ICNT = 1 only. For a steady-state run the data RIB, TMP, CONC are produced for ICNT = 0 only. The data are produced for a number of downwind distances and times as controlled by the input data in the "CLOUD" and "CALC" panels.

REFERENCES

1. Colenbrander G.W. (1980), "A mathematical model for the transient behaviour of dense vapour clouds." 3rd International Symposium on Loss Prevention and Safety Promotion in the Process Industries. Basel, September 1980.

2. Colenbrander G.W. and Puttock J.S. (1988), "Description of the HEGADAS model for dispersion of dense gas releases".

APPENDIX A. LISTING OF EXAMPLE HEGADAS INPUT DATA FILES

HEGADAS input data file TEST.HSI (steady-state run)

```
TITLE  HEGADAS-S TEST DATA
     ICNT  -      0        *                CONTOURS OR CONTENTS CODE
    ISURF  -      3        *                SURFACE TRANSFER CODE
*                           *
POOL   DATA                 *
*                           *
   PLL     -  20.           * M              SOURCE LENGTH
   PLHW    -  10.           * M              SOURCE HALF-WIDTH
*                           *
AMBIENT CONDITIONS          *
*                           *
   Z0      -  10.3          * M              REFERENCE HEIGHT
   U0      -  6.0           * M/S            WIND VELOCITY AT HEIGHT Z0
   AIRTEMP -  16.1          * DEG.CELSIUS    AIR TEMP. AT GROUND LEVEL
   RH      -  0.6           *                RELATIVE HUMIDITY
   TGROUND -  16.8          * DEG.CELSIUS    EARTH-S SURFACE TEMPERATURE
*                           *
DISP                        *
*                           *
   ROUGH   -  0.2E-03       * M              SURFACE ROUGHNESS PARAMETER
   MONIN   -  0.1E+05       * M              MONIN - OBUKHOV LENGTH
   CROSSW  -  0.064         * M**(1-BETA)    CROSSWIND (DELTA)
              0.905         *                          (BETA)
*                           *
CLOUD                       *
*                           *
   XSTEP   -  0.2           *                OUTPUT STEP LENGTH
   XMAX    -  1000.         *                X AT WHICH CALC. IS STOPPED
   CAMIN   -  0.01          * KG/M3          CA AT WHICH CALC. IS STOPPED
   CU      -  0.035         * KG/M3          UPPER CONCENTRATION LIMIT
   CL      -  0.017         * KG/M3          LOWER CONCENTRATION LIMIT
*                           *
SOURCE                      *
*                           *
   FLUX    -  0.08          * KG/M2/S        GAS EMISSION FLUX
   TEMPGAS - -161.          * DEG.CELSIUS    TEMPERATURE   OF EMITTED GAS
   CPGAS   -  34.4          * J/MOLE/'DEG.C  SPECIFIC HEAT OF EMITTED GAS
   MWGAS   -  16.04         * KG/KMOLE       MOL. WEIGHT OF EMITTED GAS
   WATGAS  -  0.            *                MOLAR FRACTION PICKED-UP WATE
*                           *
```

HEGADAS input data file TEST.HTI (transient run)

```
TITLE   HEGADAS-T TEST DATA
  ICNT     -      0          *                    CONTOURS OR CONTENTS CODE
  ISURF    -      3          *                    VERSION CODE
*
AMBIENT CONDITIONS
*
  ZO       - 10.             *   M                REFERENCE HEIGHT
  UO       - 4.              *   M/S              WIND VELOCITY AT HEIGHT ZO
  AIRTEMP  - 20.             *   C                AIR TEMP. AT GROUND LEVEL
  RH       - 0.7             *                    RELATIVE HUMIDITY
  TGROUND  - 20.             *   C                EARTH-S SURFACE TEMPERATURE
*
DISP
*
  ROUGH    - 0.007           *   M                SURFACE ROUGHNESS PARAMETER
  MONIN    - 0.1E+05         *   M                MONIN - OBUKHOV LENGTH
  CROSSW   - 0.064           *   M**(1-BETA)      CROSSWIND (DELTA)
             0.905           *                              (BETA)
*
CLOUD
*
  XSTEP    - 30.             *   M                OUTPUT STEP LENGTH
  CAMIN    - 0.0175          *   KG/M3            CA AT WHICH CALC. IS STOPPED
  CU       - 0.036           *   KG/M3            UPPER CONCENTRATION LIMIT
  CL       - 0.018           *   KG/M3            LOWER CONCENTRATION LIMIT
*
SOURCE
*
  TEMPGAS  - -42.            *   C                TEMPERATURE   OF EMITTED GAS
  CPGAS    - 68.             *   J/MOLE/'C        SPECIFIC HEAT OF EMITTED GAS
  MWGAS    - 44.1            *   KG/KMOLE         MOL. WEIGHT OF EMITTED GAS
  WATGAS   - 0.              *                    MOL. FRACT. PICKED-UP WATER
*                            *
CALC
*                            *
  TSTAR    -   120.          *
  TSTAR    -   200.          *
  TSTAR    -   280.          *
  TSTAR    -   360.          *
*                            *
SKIP  1                      *   LINES TO SKIP BETWEEN SOURCE LINES READ
*                            *
 TSTEPR-      0.200E+01      *   TIME STEP (S), & OPTIONAL MAX. RADIUS (M)
        * POOL RADIUS (M)       EVAP. RATE (KG/S)
 SOURCE-      0.401E+01   ,      0.582E+01
 SOURCE-      0.675E+01   ,      0.164E+02
 SOURCE-      0.909E+01   ,      0.298E+02
 SOURCE-      0.110E+02   ,      0.435E+02
 SOURCE-      0.126E+02   ,      0.571E+02
 SOURCE-      0.140E+02   ,      0.707E+02
 SOURCE-      0.153E+02   ,      0.841E+02
```

SOURCE-	0.164E+02	,	0.974E+02
SOURCE-	0.175E+02	,	0.111E+03
SOURCE-	0.185E+02	,	0.124E+03
SOURCE-	0.194E+02	,	0.137E+03
SOURCE-	0.203E+02	,	0.149E+03
SOURCE-	0.212E+02	,	0.162E+03
SOURCE-	0.220E+02	,	0.175E+03
SOURCE-	0.227E+02	,	0.187E+03
SOURCE-	0.235E+02	,	0.199E+03
SOURCE-	0.242E+02	,	0.211E+03
SOURCE-	0.248E+02	,	0.222E+03
SOURCE-	0.254E+02	,	0.234E+03
SOURCE-	0.260E+02	,	0.245E+03
SOURCE-	0.266E+02	,	0.256E+03
SOURCE-	0.272E+02	,	0.267E+03
SOURCE-	0.277E+02	,	0.277E+03
SOURCE-	0.282E+02	,	0.287E+03
SOURCE-	0.287E+02	,	0.297E+03
SOURCE-	0.291E+02	,	0.306E+03
SOURCE-	0.295E+02	,	0.315E+03
SOURCE-	0.299E+02	,	0.324E+03
SOURCE-	0.303E+02	,	0.332E+03
SOURCE-	0.307E+02	,	0.340E+03
SOURCE-	0.310E+02	,	0.347E+03
SOURCE-	0.313E+02	,	0.354E+03
SOURCE-	0.316E+02	,	0.360E+03
SOURCE-	0.318E+02	,	0.365E+03
SOURCE-	0.320E+02	,	0.370E+03
SOURCE-	0.322E+02	,	0.374E+03
SOURCE-	0.323E+02	,	0.377E+03
SOURCE-	0.323E+02	,	0.350E+03
SOURCE-	0.323E+02	,	0.287E+03
SOURCE-	0.323E+02	,	0.235E+03
SOURCE-	0.323E+02	,	0.192E+03
SOURCE-	0.323E+02	,	0.157E+03
SOURCE-	0.323E+02	,	0.129E+03
SOURCE-	0.323E+02	,	0.106E+03
SOURCE-	0.323E+02	,	0.864E+02
SOURCE-	0.323E+02	,	0.707E+02
SOURCE-	0.323E+02	,	0.579E+02
SOURCE-	0.323E+02	,	0.474E+02
SOURCE-	0.323E+02	,	0.388E+02
SOURCE-	0.323E+02	,	0.318E+02

Table Ia. HEGADAS input data (steady-state)

Keyword	Symbol	Min.	Max.	Ref.	Units	Meaning
TITLE	(alphanumeric value: title)					**PANEL - CONTROL PARAMETERS**
ICNT	-	0	1	-	-	0 - output Richardson numbers, temperature and gas volume concentration 1 - output cumulative cloud volume/mass data
ISURF	-	2	4	2(5.1) 2(5.2)	-	2 - NO surface heat transfer or water vapour flux 3 - include surface heat transfer 4 - include surface heat transfer and water vapour flux
POOL						**PANEL - POOL GEOMETRY**
PLL	L_p	10^{-3}	999999	1	m	primary source length
PLHW	B_p	10^{-3}	999999	1	m	primary source half-width
AMBIENT						**PANEL - AMBIENT CONDITIONS**
AIRTEMP	T_a	-50	50	2(A)	°C	air temperature at ground level
RH	r_H	0	1	2(A)	-	relative humidity of air (default r_H=0)
UO	u_0	1.5	20	2(3.1)	m/s	wind speed at reference height
ZO	z_0	0.1	50	2(3.1)	m	reference height
TGROUND	T_s	-50	50	2(5.1)	°C	ground temperature
DISP						**PANEL - DISPERSION DATA**
ROUGH	Z_R	10^{-6}	10	2(3.1)	m	surface roughness parameter (Table III-I)
MONIN	L_M	-500	10^4	2(3.1)	m	Monin-Obukhov length (see Fig. 1)
CROSSW	δ	0.02	0.6	2(4.1)	$m^{1-\beta}$	) constants in power-law $S_y = \delta x^\beta$ for
	β	0.8	1.0	2(4.1)	-	) cross-wind dispersion coefficient (see Table
						) III-2; defaults δ = 0.064, β = 0.905)
CE	C_E	1.0	1.3	2(4.1)	-	constant in gravitational spreading law (default C_E = 1.15)

Table Ia. (continued)

Keyword	Symbol	Min.	Max.	Ref.	Unit	Meaning
SOURCE						**PANEL - SOURCE/GAS DATA**
FLUX	Q_p	10^{-7}	1	2(4.2)	$kg/m^2/s$	(dry) gas evaporation flux, source strength
TEMPGAS	T_p^g	-270	100	2(A)	°C	source gas temperature
CPGAS	C_{pg}^g	5	200	2(A)	J/mol/K	specific heat of gas
MWGAS	M^{pg}	2	200	-	kg/kmol	molecular weight of gas
WATGAS	ω_2^g	0	0.2	2(5.2)	-	molar ratio of water initially in gas (picked up) to dry gas; default ω_2'=0
HEATGR	-	5	100	2(5.1)	-	heat group in natural convection heat flux (default methane: HEATGR=24)
DISTS	x_s	0	99999	-	m	**PANEL - BREAKPOINT DATA** - optional- downwind x co-ordinate at which break-point data are specified.
			SPECIFY EITHER HS OR CONCS			
HS	H_{eff}	0	99999	2(3.1)	m	specified height of cloud, $H_{eff} = H_{eff}(x_s)$
CONCS	y_{wg}	0	1	2(A)	-	specified ground level concentration on plume axis (molar fraction of wet gas).
TMPS	T_m	-270	50	2(5.1)	°C	specified cloud temperature (only if CONCS is also specified; optional)
WS	b	0	99999	2(4.1)	m	specified half-width of cloud; optional
CLOUD						**PANEL - OUTPUT CONTROL DATA**
XSTEP	-	0.01	10	-	-	ratio of initial downwind step length to secondary source length, L
XMAX	-	1.0	99999	-	-	ratio of X-co-ord. at which calculation stops, to secondary source length L
CMIN	-	10^{-7}	5	-	kg/m^3	ground level plume axis concentration at which calculation stops
CU	c_U	10^{-7}	5	-	kg/m^3)	upper and lower concentration limits;
CL	c_L	10^{-7}	5	-	kg/m^3)	output of isoconcentration contours $c = c_U$) and $c = c_L$, and cumulative cloud data

Table Ib. HEGADAS input data (transient run)

Keyword	Symbol	Min.	Max.	Ref.	Unit	Meaning
TITLE	(alphanumeric value: title)					**PANEL - CONTROL PARAMETERS**
ICNT	-	0	1	-	-	0 - output Richardson numbers, temperature and gas volume concentration 1 - output cumulative cloud volume/mass data
ISURF	-	2	4		-	2 - NO surface heat transfer or water vapour flux 3 - include surface heat transfer 4 - include surface heat transfer and water vapour flux
				2(5.1) 2(5.2)		
BLANKET	(alphanumeric value: 'ONLY')					optional; if included, the calculations in HEGADAS are limited to source conditions, initial gas blanket, and no dispersion calculations are made
AMBIENT						**PANEL - AMBIENT CONDITIONS**
AIRTEMP	T_a	-50	50	2(A)	°C	air temperature at ground level
RH	r_H	0	1	2(A)	-	relative humidity of air (default r_H=0)
UO	u_0	1.5	20	2(3.1)	m/s	wind speed at reference height
ZO	z_0	0.1	50	2(3.1)	m	reference height
TGROUND	T_s	-50	50	2(5.1)	°C	ground temperature
DISP						**PANEL - DISPERSION DATA**
ROUGH	Z_R	10^{-6}	10	2(3.1)	m	surface roughness parameter (Table III-I)
MONIN	L_M	-500	10^4	2(3.1)	m	Monin-Obukhov length (see Fig. 1)
CROSSW	δ	0.02	0.6	2(4.1)	$m^{1-\beta}$	constants in power-law $S_y = \delta x^\beta$ for
	β	0.8	1.0	2(4.1)	-	cross-wind dispersion coefficient (see Table III-2; defaults δ = 0.064, β = 0.905)
CE	C_E	1.0	1.3	2(4.1)	-	constant in gravitational spreading law (default C_E = 1.15)
SOURCE						**PANEL - SOURCE/GAS DATA**
TEMPGAS	T_s	-270	100	2(A)	°C	source gas temperature
CPGAS	$C_s^{P_s}$	5	200	2(A)	J/mol/K	specific heat of gas
MWGAS	M^{P_s}	2	200	-	kg/kmol	molecular weight of gas
WATGAS	ω_2^s	0	0.2	2(5.2)	-	molar ratio of water initially in gas (picked up) to dry gas; default ω_2'=0
HEATGR	-	5	100	2(5.1)	-	heat group in natural convection heat flux (default methane: HEATGR=24)

Table Ib. (continued)

Keyword	Symbol	min.	max.	Ref.	Unit	Meaning
DISTS	x_s	0	99999	-	m	**PANEL - BREAKPOINT DATA** - optional- downwind x co-ordinate at which break-point data are specified
		SPECIFY EITHER HS OR CONCS				
HS	H_{eff}	0	99999	2(3.1)	m	specified height of cloud, $H_{eff} = H_{eff}(x_s)$
CONCS	-	0	1	2(A)	-	specified multiplification factor of calculated ground level concentration y_{wg} on plume axis (molar fraction of wet gas): CONCS = $y_{wg}^{new}(x_s) / y_{wg}^{old}(x_s)$
CLOUD						**PANEL - OUTPUT CONTROL DATA**
XSTEP	-	0.1	9999	-	m	output step length
CMIN	-	10^{-7}	5	-	kg/m^3	ground level plume axis concentration at which calculation stops
SIGX	a_x	0.01	1	1	m^{1-n}	) constants in power-law, $S_z = a_x x^n$ for the
	b_x	0.8	1.2	2(6.2)	-	) down-wind dispersion coefficient, $n=b_x$
						) (default values a_x=0.13, b_x=1.0
CU	c_U	10^{-7}	5	-	kg/m^3	) upper and lower concentration limits;
CL	c_L	10^{-7}	5	-	kg/m^3	) output of isoconcentration contours $c = c_U$
						) and $c = c_L$, and cumulative cloud data
CALC			**PANEL - OUTPUT OF TIMESTEPS**			
TSTAR	-	1	999999	-	s	output times for which cloud conditions are to be calculated (maximum of 20 times)
SKIP		0	99	-		**PANEL - POOL DATA** the SKIP value is an integer. If set to zero every SOURCE record is read, if set to one every second record, etc
TSTEPR	Δt	0	100	-	s	) data on one record: size of time step and
	-	0	9999	-	m	) optional (for bunds only) bund radius
SOURCE	R_i	0	9999	-	m	) data on one record (maximum number of 9999
	E_i	0	999999		kg/s	) records): pool radius, evaporation flux of
	-	0	999999	-	m	) dry gas, and optional (for bunds only)
						) vapour height

TABLE IIa. HEGADAS - output data- Steady State Model

Symbol	Unit	Meaning
DISTANCE	m	downwind distance from source (x co-ordinate) for current calculation step, x_p.
CA	kg/m^3	ground level concentration on plume axis, c_A (dry gas)
SZ	m	vertical dispersion coefficient, S_z.
SY	m	cross-wind dispersion coefficient, S_y.
MIDP	m	half-width $b = b(x_p)$ of the middle part of the cross-wind concentration profile, see fig. 1 of Ref. 1.
YCU, YCL	m	y - co-ordinate (i.e. cross-wind distance to the plume axis) at which a ground level concentration equal to CU or CL respectively is predicted (CU, CL are specified in "CLOUD")
ZCU, ZCL	m	height at which a concentration equal to CU or CL respectively is predicted on the cloud centerline.
VCU, VCL	m^3	volume of the cloud where C>CU, or C>CL, for the part of the cloud up to $x = x_p$
MCU, MCL	kg	vapour content of the cloud where C>CU, or C>CL, for the part of the cloud up to $x=x_p$
RIB	-	bulk Richardson number Ri_*
TMP	°C	ground level plume axis temperature
CONC	-	ground level plume axis concentration (% volume dry gas)

TABLE IIb. HEGADAS - output data - Transient Model

Symbol	Unit	Meaning
X	m	downwind distance from source for which data of the current output step are produced (m), x_p
CA	kg/m^3	ground level concentration on the plume axis, c_A (dry gas)
SZ	m	vertical dispersion coefficient at x_p , S_z
SY	m	cross-wind dispersion coefficient at x_p, S_y
MIDP	m	half-width, b, of the middle part of the concentration profile at x_p
YCU, YCL	m	cross-wind distances of the isoconcentration contours for CU, CL from the plume axis, evaluated at ground level.
ZCU, ZCL	m	heights of the isoconcentration contours for CU, CL on the plume axis
CONC	-	ground level concentration on the plume axis, %volume
CUM.VOL	m^3	Cumulative volume of the cloud (up to position x_p) where C > CU and C > CL.
CUM.CONT	kg	Cumulative mass of the gas (up to position x_p) where C > CU and C > CL.

TABLE III – 1

VALUES OF THE SURFACE ROUGHNESS PARAMETER z_R

(Ref. ESDU, Engineering Sciences Data Item No. 74031 (1974b))

Stability Class (Pasquill)	$\delta_{10\ min}$	δ_I	β
A	0.527	0.264	0.865
B	0.371	0.186	0.866
C	0.209	0.105	0.897
D	0.128	0.064	0.905
E	0.098	0.049	0.902
F	0.065	0.033	0.902

Table III-2. Constants in experimentally determined crosswind dispersion coefficient for a point source $S_y = \delta x^{\beta}$
$\delta_{10\ min}$ are the values for an averaging time for the concentration measurmeent of 10 min. If the averaging time is t sec. δ_t can be calculated, using the following formula:

$$\delta_t = \delta_{10\ min} \left(\frac{t}{600}\right)^{0.2}$$

The values for δ_I apply to instantaneous sources; these values are recommended for use in dispersion calculations for flammable gases.

Source: "Methoden voor het berekenen van de gevolgen van het vrijkomen van gevaarlijke stoffen". TNO, 2nd ed.

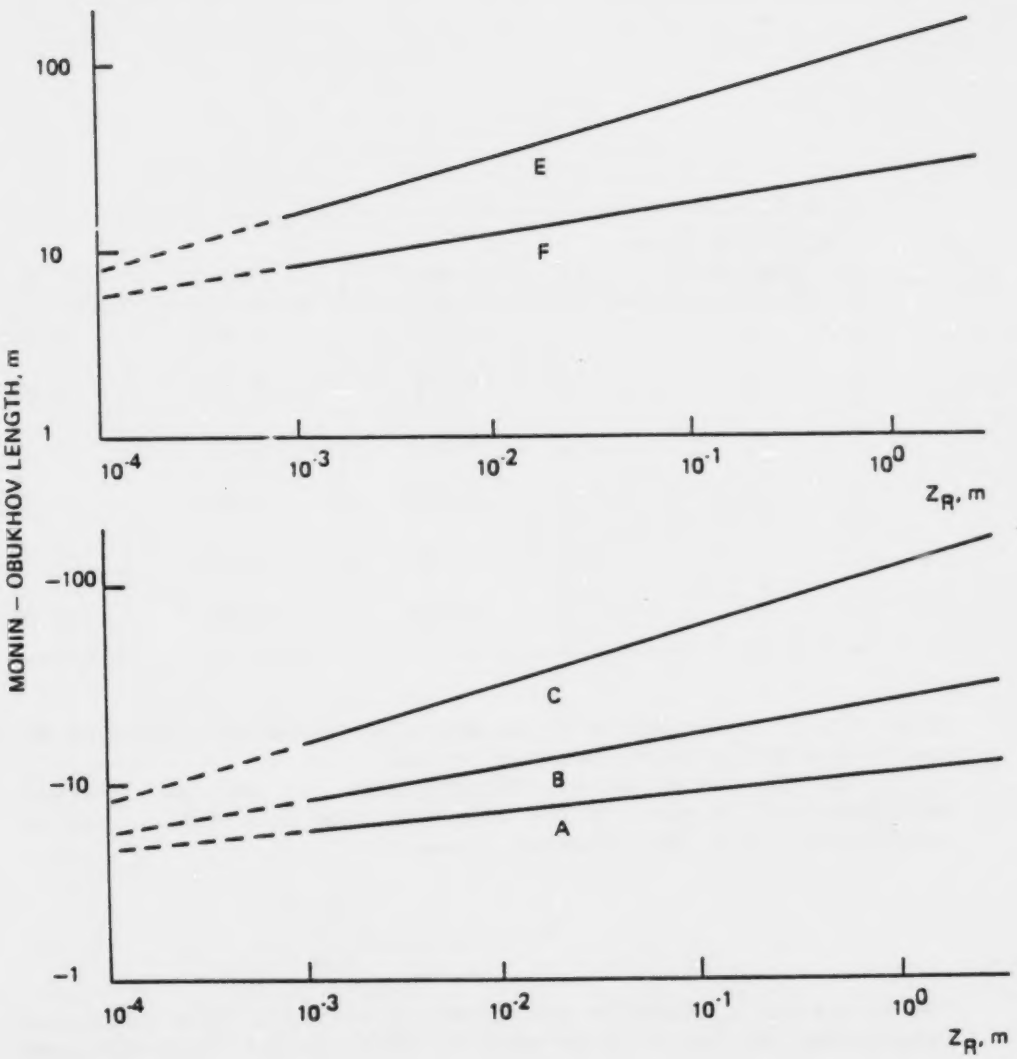

For Class D, L_m approaches ∞.

FIG. 1 – The Monin-Obukhov length as a function of Pasquill stability class and surface roughness length z_R (Ref. J.S. Irwin, Technical Note, Atmos. Env. 13, 1979)

APPENDIX B

DISPERSION OF RELEASES OF DENSE GAS: DEVELOPMENT OF THE HEGADAS MODEL

by

G.W. Colenbrander and J.S. Puttock

Koninklijke/Shell Laboratorium Amsterdam

CONTENTS

1. Introduction 3

2. Similarity profiles 5

3. Vertical mixing 6
   3.1. The vertical dispersion coefficient S_z
   3.2. Entrainment rates determined in a wind tunnel
   3.3. Annular entrainment studies in the laboratory
   3.4. Entrainment rates determined in a wind flume
   3.5. The entrainment relation used in HEGADAS for stable stratification
   3.6. Vertical dispersion in an unstable atmosphere

4. Gravity spread and lateral mixing 17
   4.1. The cross-wind dispersion coefficient S_y
   4.2. The ground level centre line concentration c_A
   4.3. Sources with time-dependent vapour emission rate and/or dimensions

5. Thermal effects 25
   5.1. Heat transfer from the surface
      5.1.1. Theory
      5.1.2. Experimental test
   5.2. Transfer of water vapour from a water surface into the cloud
   5.3. Convective entrainment

6. The time-dependent model 35
   6.1. The transient dispersion model
   6.2. Dispersion in the wind direction
   6.3. Solution of the equations
   6.4. Instantaneous gas release

7. Comparison with experiment 41

8. Conclusions 42

References 43

Appendices 46

A. The thermodynamics of a mixture of evaporating liquefied gas, moist air and entrained water. Calculation of temperature and density in subroutine THERMO
   A.1. Introduction
   A.2. Notation
   A.3. Thermodynamic equations
   A.4. Empirical function for water vapour pressure
B. Wind velocity and observer velocity
   B.1. The wind velocity profile
   B.2. Relation of observer velocity to wind velocity
C. Cloud shape correction for gravitational spreading in the wind direction
D. Laboratory experiments on heat and mass transfer into a cold nitrogen gas flow
E. Summary of HEGADAS equations

Table

Figures

DISPERSION OF RELEASES OF DENSE GAS: DEVELOPMENT OF THE HEGADAS MODEL

1. INTRODUCTION

In assessing the potential hazards associated with industrial installations, it is often necessary to consider the possible consequences of the accidental release of flammable or toxic gases. As part of this assessment, calculations of their dilution in the atmosphere are required. For this, mathematical models of gas dispersion are needed. Many such gases, either by virtue of their molecular weight or low temperature, are denser than air when released. The dispersion of such dense clouds is qualitatively, as well as quantitatively, different from the behaviour of neutrally buoyant releases. Hence there has been considerable interest in recent years in the development of our understanding of dense gas dispersion, and of models for this process.

Dense-gas dispersion models tend to fall into two categories (although there are a few with an intermediate status). Most complex are three-dimensional grid solutions of sets of partial differential equations which represent, at some level of turbulence closure, approximations to the averaged Navier-Stokes equations. These models have the prospect of eventually being able to deal with such complexities as flow around obstacles. However, their application to such flows is still under development and is likely to require larger-scale computing facilities than are generally available today. The other main category comprises integral models, which take assumed profile shapes and solve ordinary differential equations for such parameters as height and width of the cloud. Some empirical input is required, for example, to determine relations for the

entrainment of air into the cloud. It seems that the best of such models can predict dispersion over flat surfaces at least as well as the more complex models, and at much lower computational cost.

The model HEGADAS is an example of the latter type. It uses forms of concentration profile that can be used without a need for sudden change into the region of passive dispersion. The basic model was described by Colenbrander(1980). Since then a number of changes have been made to HEGADAS. Some, such as heat transfer, were clearly necessary additions for the proper description of dispersion of materials such as LNG. The need for inclusion of water vapour transfer, by contrast, only becomes clear as a result of the analysis of field data. Some further changes have been made as a result of a better understanding of laboratory experiments.

This report contains a full description of the formulation of the steady-state version of HEGADAS, with these changes included. The validation of the model against field data is the subject of a number of papers (Puttock et al., 1982, 1984, Colenbrander and Puttock, 1984, Puttock, 1987).

2. SIMILARITY PROFILES

The following similarity profiles for the time-mean wind velocity u_x in the atmospheric surface layer and for the vapour concentration c in the heavy gas plume are adopted:

$$u_x = u_o \left(\frac{z}{z_o}\right)^{\alpha} \qquad \ldots (2.1)$$

$$c(x,y,z) = c_A(x)\exp\left[- \left(\frac{|y| - b(x)}{S_y(x)}\right)^2 - \left(\frac{z}{S_z(x)}\right)^{1+\alpha} \right] \quad \text{for } |y| > b$$

$$\ldots (2.2)$$

$$c(x,y,z) = c_A(x)\exp\left[- \left(\frac{z}{S_z(x)}\right)^{1+\alpha} \right] \quad \text{for } |y| < b$$

The x-direction in the Cartesian coordinate system coincides with the wind direction (see Figure 1); the y and z directions are the horizontal and vertical crosswind directions respectively. The z = 0 plane represents the earth's surface and the y = 0 plane is the plane of symmetry of the vapour plume. The similarity profiles used are illustrated in Figure 1.

3. VERTICAL MIXING

3.1 The vertical dispersion coefficient S_z

The vertical concentration distribution

$$c(x,z) = c_A(x)\exp\left[- \left(\frac{z}{S_z(x)}\right)^{1+\alpha} \right] \qquad \ldots(3.1)$$

must satisfy the simple two-dimensional diffusion equation

$$u_x \frac{\partial c}{\partial x} = \frac{\partial}{\partial z}\left(K_z \frac{\partial c}{\partial z}\right) \qquad \ldots(3.2)$$

where the turbulent diffusivity K_z is given by

$$K_z = \frac{k u_* z}{\Phi\,(Ri_*)} \qquad \ldots(3.3)$$

In this expression the variable u_* is the friction velocity, $k = 0.41$ the von Karman constant and Ri_* a bulk Richardson number.

The function $\Phi(Ri_*)$ describes the influence of a density stratification on the diffusion in the vertical direction and is obtained from experimental data as we will show later in sections 3.2 - 3.6; the bulk Richardson number Ri_* which quantifies the density stratification, is defined below (Equation 3.6).

Substituting equations (2.1), (3.1) and (3.3) into equation (3.2), and making use of the conservation of mass flux ($\int_0^\infty c u_x \, dz = \text{constant}$) we find that in the two-dimensional case the dispersion coefficient $S_z(x)$ can be determined from the following ordinary differential equation:

$$\frac{d}{dx}\left(\frac{S_z}{z_o}\right)^{1+\alpha} = \frac{k}{z_o}\frac{u_*}{u_o}(1+\alpha)^2/\Phi(Ri_*) \qquad \ldots(3.4)$$

The ratio $\frac{u_*}{u_o}$ is obtained from the logarithmic wind velocity profile (Businger, 1973):

$$\frac{u_*}{u_o} = k \left[\ln \left(\frac{z_o + z_R}{z_R} \right) - \psi_1 \left(\frac{z_o}{\lambda} \right) \right]^{-1} \qquad \ldots(3.5)$$

where ψ_1 is defined in Appendix B. For a given reference height z_o this ratio depends on the two length scales z_R, the roughness length, and λ, the Monin-Obukhov length.

We define the bulk Richardson number Ri_* as follows:

$$Ri_* = g \frac{\Delta\rho}{\rho_a(z=o)} \frac{H_{*ff}}{u^2_*} \qquad \ldots(3.6)$$

where g is the gravitational acceleration and $\rho_a(z=0)$ the air density at ground level.

The effective height of the plume, H_{*ff}, is defined as:

$$H_{*ff} = \frac{1}{c_A} \int_0^\infty c\,dz = \frac{\Gamma\left(\frac{1}{1+\alpha}\right)}{1+\alpha} S_z \qquad \ldots(3.7)$$

The density difference $\Delta\rho$ is defined as:

$$\Delta\rho = \rho_m(c=c_A) - \rho_a(z=H_{*ff}) \qquad \ldots(3.8)$$

In this case expression $\rho(c=c_A)$ denotes the density of a mixture of gas with concentration c_A and ambient air.

The horizontal transport velocity of the emitted gas in the plume, averaged over the plume height, is given by:

$$u_{*ff} = \frac{\int_0^\infty u_x c\,dz}{\int_0^\infty c\,dx} \qquad \ldots(3.9)$$

Using for u_x and c expressions (2.1) and (2.2b) we find:

$$u_{*ff} = \left(\frac{S_z}{z_0}\right)^{\alpha} \frac{1}{\Gamma\left(\frac{1}{1+\alpha}\right)} u_0 \qquad \ldots(3.10)$$

The entrainment velocity u_* of air into the plume is given by:

$$u_* = \frac{d}{dx}\left(u_{*ff}\, H_{*ff}\right) \qquad \ldots(3.11)$$

which, using expressions (3.7) and (3.10) for H_{*ff} and u_{*ff}, can be expressed as:

$$u_* = \frac{u_0}{z_0^{\alpha}(1+\alpha)} \frac{d}{dx} S_z^{1+\alpha}$$

Then, making use of Equation (3.4) we find for the entrainment velocity:

$$u_* = (1+\alpha)\, k u_* / \Phi(Ri_*) \qquad \ldots(3.12)$$

Equation (3.4) describes the entrainment of air into the plume if the plume width is constant, so that the problem is two-dimensional. This condition does not hold for a dense vapour plume, which will spread laterally due to the density difference with the surrounding air. For this case, Equation (3.4) has been generalised into

$$\frac{d}{dx}\left[B_{*ff} \left(\frac{S_z}{z_o}\right)^{1+\alpha} \right] = \frac{k}{z_o} \frac{u_*}{u_o} (1+\alpha)^2 B_{*ff} / \Phi(Ri_*) \qquad \ldots(3.13)$$

The variable B_{*ff} is the effective half-width of the plume, defined by

$$B_{*ff} = b + \frac{\sqrt{\pi}}{2} S_y \qquad \ldots(3.14)$$

This definition has been chosen because integration of the similarity profile for the concentration (Equation 2.2) in the y-direction gives

$$\int_0^{\infty} c(x,y,z)\, dy = c_A \left(b + \frac{\sqrt{\pi}}{2} S_y \right) \exp\left[- \left(\frac{z}{S_z}\right)^{1+\alpha} \right]$$

The crosswind gravity-spreading of the plume is discussed in Section 4.

3.2 Entrainment rates determined in a wind tunnel

The entrainment function $\Phi(Ri_*)$ is determined from laboratory data. A variety of laboratory experiments on entrainment through density interfaces appear to be relevant.

Britter (1980) analysed the experiments carried out by McQuaid (1976) in a 29 m long wind tunnel with a width of 0.3 m. Dense carbon dioxide gas was introduced 16 m from the entrance at the bottom of the tunnel through a 0.3 x 0.05 m porous plate. Measurements of velocity and concentration were made up to 5 m downwind of the centreline of the source. From a measured ground level concentration c_A, Britter defined the local heavy gas layer height H as:

$$H = \frac{\rho_o \, q_o}{c_A \, u} \qquad \ldots(3.14)$$

where ρ_o is the density of the emitted carbon dioxide and q_o the source strength (in m^3/s per meter tunnel width) and u is the mean velocity in the tunnel ($\approx 0.8 \, u_{max}$). When ρ and ρ_a are the densities of the gas mixture and air, respectively, we can write:

$$\rho = c_A + (1 - \frac{c_A}{\rho_o}) \, \rho_a \qquad \ldots(3.15)$$

and

$$\Delta\rho = \rho - \rho_a = c_A \frac{\rho_o - \rho_a}{\rho_o} = c_A \frac{\Delta\rho_o}{\rho_o} \qquad \ldots(3.16)$$

Using the bulk Richardson number $Ri_B = g \frac{\Delta\rho}{\rho_a} \frac{H}{u^2}$, in which we substitute

Equations (3.14) and (3.16) for H and $\Delta\rho$, we obtain:

$$Ri_B = g \frac{\Delta\rho_o}{\rho_a} \frac{q_o}{u^3} = \text{constant} \qquad \ldots(3.17)$$

From the experimental data Britter determined the entrainment rate u_e/u as a function of this bulk Richardson number, Ri_B. McQuaid gives $(u_*/u)^2 = 1.7 \times 10^{-3}$ in the working section of the tunnel in the absence of any dense fluid and hence we find: $Ri_* = Ri_B/0.0017$ and $u_e/u_* = 24.3 \times (u_e/u)$. This dimensionless entrainment rate u_e/u_* as a function of Ri_* is given in Figure 2 (McQuaid data points).

3.3 Annular entrainment studies in the laboratory

In several publications results are given of experiments on interfacial mixing between a heavy fluid layer and a light fluid layer on top of it. The best resemblance with atmospheric dispersion under stably stratified conditions with wind is observed in experiments where the turbulence is supported by a shear flow. Such a flow is generated either by a surface stress acting on the upper layer (Kantha et al., 1977, Kato and Phillips, 1969) or by horizontal jets, either in the top layer (Ellison and Turner, 1959) or in the bottom layer (Lofquist, 1960, Moore and Long, 1971). The experimental results on interfacial mixing are presented in the form of a non-dimensional entrainment velocity as function of a bulk Richardson number.

The experiments of Kantha, Phillips and Azad (1977) (hereafter KPA) were conducted in an annular tank. A constant stress $\tau = \rho u_*^2$ was applied by a rotating screen at the surface of a stratified fluid consisting of a light upper layer and a heavy bottom layer. The depth H of the mixed upper layer and the screen velocity were observed in time.

The initial condition consisted of two layers with uniform densities and a density difference $\Delta\rho_o$. During an experiment the density of the upper layer appeared to remain uniform and increased with increasing layer depth H; the density of the bottom layer remained at its initial value. The bulk Richardson number Ri_* remained constant during an experimental run, and the entrainment velocity u_* was derived from the observations of the rate of change of H. The results were found to be dependent on the channel width W owing to side-wall effects. Observations over a range of values of H/W were therefore extrapolated to H/W = 0.

The entrainment relation used originally in HEGADAS was based in part on the KPA data. However, further experiments with annular tanks have shown that the results are not directly applicable. Deardorff and Willis (1982) reported results of a new set of rotating screen annnulus experiments. Their analysis of these and other experiments on entrainment in stably stratified conditions suggests a better collapse of the data when not only Ri_* is used as scaling parameter, but also Ri_v, a Richardson number based on the velocity jump across the interface between the two fluid layers. Scranton and Lindberg (1983) used density and velocity probes to study in more detail flow pattern and entrainment in their rotating screen experiments. They found an extremely inhomogeneous distribution of turbulence energy over the radius of the annulus with very high turbulence levels close to the outer wall. From their observations they derived a conceptual flow model as given in Figure 3. They concluded that these experiments show a complex three-dimensional, nonhomogeneous flow with secondary motions due to channel curvature. Entrainment was observed to occur only in the outer portion of the interface. Figure 4 indicates the experimental variability in annular entrainment studies.

Although it is a simplistic representation of the experiments, involving many parameters, it serves as an illustration that results differ widely depending on experimental details.

3.4 Entrainment rates determined in a wind flume

Kranenburg (1984) studied entrainment rates between stably stratified water layers in a wind flume. The flume contained two water layers: a dense bottom layer and a light top layer of fresh tap water. The relative density difference, varying from 0.005 to 0.039 was obtained by sodium chloride, dissolved in the bottom layer. The initial depth of the upper layer was 0.10 m in all experiments. A fan sucked air through an air intake constructed at the upstream end wall. The air velocities at 0.1 m above the water surface varied from 4 to 11 m/s. The shear stress exerted by the air flow on the water surface was determined from measured velocity profiles in air and water and from pressure-difference measurements in the air. The three methods produced consistent values of u_*. The presence of the end walls limits the duration of an experiment since the surface shear stress generates an accelerating mean flow in the wind direction in the top layer and a flow against the wind in the bottom layer. It was necessary to extend the duration of the experiments at larger values of Ri_* since the time for the entrainment process to become fully developed increases and the entrainment rate decreases, as Ri_* increases. In the larger Ri_* experiments the water transported in the upper layer was selectively withdrawn with an adjustable skimmer valve at the downstream end, pumped back and discharged smoothly at the upstream end. Kranenburg corrected the results of the entrainment experiments for some additional mixing caused by this procedure.

Entrainment rates u_e of dense fluid into the top layer were determined from the rate of increase of the top layer depth H, read from filmed shadowgraph images: $u_e = dH/dt$. In the fully developed encrainment process the Richardson number $g \frac{\Delta\rho}{\rho} \frac{H}{u_*^2}$ is constant and hence the entrainment rate is also constant. The dimensionless entrainment rates u_e/u_*, measured by Kranenburg are given in Figure 2.

3.5 The Entrainment relation used in HEGADAS for stable stratification

For entrainment of air into a heavy gas layer at ground level we return to Equation (3.12).

$$u_e = (1+\alpha)\, k u_*/\Phi(Ri_*)$$

For the determination of the function $\Phi(Ri_*)$ we have used the experimental data of McQuaid and Kranenburg discussed above. The geometry of the McQuaid experiments very well simulated atmospheric plume dispersion, but the Richardson numbers in large heavy gas emissions at low wind speed conditions may exceed the range of these experiments. For high Richardson numbers we fitted our entrainment relation to the Kranenburg data, which agree well with McQuaid's data for overlapping Richardson numbers. For large values of Ri_* the entrainment rates measured by Kranenburg are substantially larger than the data from the annular entrainment experiments discussed in Section 3.3. However, Price (1979) and Thompson (1979) extrapolated the KPA results to zero aspect ratio and found $u_e/u_* = (0.8 \pm 0.1)\, Ri_*^{-1/2}$. This $Ri_*^{-1/2}$ behaviour was also predicted by several numerical models (Kranenburg, 1984) and is in good agreement with the Kranenburg data. Originally the HEGADAS entrainment relation was based on the KPA data for large Ri_* (Colenbrander, 1980). In view of the large uncertainties associated with the annular entrainment

experiments due to curvature, substitution of this relation by one based on the Kranenburg data seems justified.

The Φ - function now reads:

$$\Phi(Ri_*) = (1.0 + 0.8\ Ri_*)^{1/2} \text{ for } Ri_* > 0 \qquad \ldots(3.18)$$

Graphical representations of u_*/u_*, expressed in (3.12) and (3.18), are given in Figure 2 for $\alpha = 0.1$ and 0.7. In theory the value of α may vary between zero and one but in almost all applications of the model the possible range will be from 0.1 (very low surface roughness; neutral atmospheric stability) to 0.7 (high surface roughness; stable atmosphere).

As a consequence of the definition of $\Delta\rho$, the formulation is equally applicable to the dispersion of a trace gas in a stable ambient atmosphere, where $\Delta\rho > 0$ owing to the ambient density gradient. It remains to be seen whether it provides a good description of such dispersion with Φ given by (3.18). This is covered in Section 3.6 below.

Two comments can be made in relation to the adoption of equation (3.18). First, it is more conventional to use an expression where $\Phi \sim Ri_*^{-1}$ for large Ri_*, rather than $\Phi \sim Ri_*^{-\frac{1}{2}}$. However, most of the experiments which have been used to support Ri_*^{-1} have been experiments without mean shear (e.g. Turner, 1968), or those, such as KPA, where the initial simple interpretation has been shown to be inappropriate. As emphasised by Britter (1988) the mechanisms of entrainment through strong density gradient can be different when driven by mean shear rather than by external turbulence. In the same paper, Britter suggests that even the McQuaid data are approaching a Ri_*^{-1} asymptote at the largest Ri_*; however, the data in fact fit the $Ri_*^{-\frac{1}{2}}$ asymptote of Equation (3.18) just as well, if not better.

Second, we agree with the contention of Britter (1988) that dense gas releases, when not constrained laterally, spread so that Ri_* very rapidly reaches the range of the McQuaid data. Thus the form of the Φ function for larger values of Ri_* may be almost irrelevant in practical terms. This is consistent with our observation that changing to equation (3.18) from the previous relation based on KPA has made very little difference to practical dispersion predictions.

3.6 Vertical dispersion in an unstable atmosphere

For non-neutral atmospheric stability the value of $\rho_a(z = H_{eff})$ in Equation (3.8) is obtained from Businger's (1975) relation for the potential temperature in the atmospheric surface layer, given the roughness length z_R, the Monin-Okubkhov length λ, the friction velocity u_* and the air temperature at ground level. For unstably stratified conditions ($Ri_* < 0$), we have arranged $\Phi(Ri_*)$ to be compatible with the results of the Prairie Grass tracer dispersion experiments.

In the Prairie Grass Project, sulphur dioxide was released as a tracer from a steady-state point source at a height of 0.46 m. Concentrations were measured at a height of 1.5 m along arcs at distances of 50 m, 100 m, 400 m and 800 m from the source. We used the experimental data presented by Horst (1979). He calculated a normalised concentration $u_*\chi/E$ by dividing the crosswind-integrated concentration $\chi(z=1.5m)$ by the source strength E, and multiplying it by the friction velocity u_*. The experimental values as a function of $1/\lambda$ are shown as dots in Figure 5. Positive values of λ correspond to stable atmospheric conditions, negative values of λ to unstable ones. Horst used Businger's (1973) relations for the vertical profiles of wind velocity and temperature and fitted them to the observed profiles to estimate the Monin-Obukov length λ for a height of

2 m and the friction velocity u_* for each diffusion experiment; the roughness length he used was $z_R = 0.6$ cm.

The open symbols in Figure 5 denote cases where the computed λ varied by more than a factor of 2 between heights of 1 m and 4 m. This indicates that Businger's relations were not compatible with the observed profiles of wind velocity and temperature.

By choosing

$$\Phi(Ri_*) = (1 - 0.6\ Ri_*)^{-0.5} \qquad \ldots(3.19)$$

for unstable conditions (Ri_* and $\lambda < 0$) a good fit between the HEGADAS calculations and the Prairie Grass data was obtained, as is shown by the curve in Figure 5. Figure 5 also shows that the data for stable conditions are well predicted using Φ as in Equation (3.18).

Expression (3.19) is used in the model calculations whenever Ri_* becomes negative, irrespective of whether it is due to cloud buoyancy or to unstable atmospheric stratification.

4. GRAVITY SPREAD AND LATERAL MIXING

4.1 The cross-wind dispersion coefficient S_y

The crosswind dispersion coefficient S_y is determined in a way very similar to the method described by te Riele (1977). Consider first the widely used crosswind concentration distribution

$$c = c_A \exp\left(-\tfrac{1}{2}\left(\frac{y}{S_y}\right)^2\right) \qquad \ldots(4.1)$$

Experimental data on crosswind dispersion from ground level point sources have been collected in the Gifford-Pasquill system (Turner, 1969), this giving the crosswind dispersion coefficient σ_y as a function of the downwind distance.

This dependence may be well approximated by a power law.

$$S_y = \delta\, x^{\beta}$$

To extend this to our similarity profile with uniform mid-part, note that, if we assume that the turbulent crosswind diffusion coefficient K_y is directly proportional to the wind velocity u_x and the half-width of the concentration profile W (to be defined later) to some power γ, such that

$$K_y = K_o\, u_x\, W^{\gamma}, \qquad \ldots(4.2)$$

Making use of the conservation of maxx flux ($\int_0^{\infty} c\, u_x\, dz$ = constant) it is now easily shown that (4.1) satisfies the simple two-dimensional diffusion equation

$$u_x \frac{\partial c}{\partial x} = \frac{\partial}{\partial y}\left(K_y \frac{\partial c}{\partial y}\right) \qquad \ldots(4.3)$$

provided that

$$S_y \frac{dS_y}{dx} = K_o W^{\gamma} \qquad \ldots(4.4)$$

Equation (4.4) is satisfied by a crosswind half-width W of

$$W = \sqrt{\pi}/2 \; S_y ; \qquad \ldots(4.5)$$

we then find that $\gamma = 2 - \frac{1}{\beta}$ and $K_o = \frac{2\beta}{\pi} \left(\delta \sqrt{\pi}/2 \right)^{1/\beta}$

If the middle part b in the similarity profile for the concentration (Equation (2.2)) is zero, Equation (4.4) is equivalent to

$$S_y \frac{dS_y}{dx} = \frac{4\beta}{\pi} W^2 \left(\frac{\delta\sqrt{\pi}/2}{W} \right)^{\frac{1}{\beta}} \qquad \ldots(4.6)$$

where

$$W = \frac{\sqrt{\pi}}{2} S_y$$

In the heavy gas dispersion model we assume that equation (4.6) also holds true if b is not zero. For this case we define the profile half-width W as

$$W = b + \frac{\sqrt{\pi}}{2} S_y \qquad \ldots(4.7)$$

A dense vapour plume will spread laterally due to the difference in density between it and the surrounding air. This gravitational spreading is taken into account with the simple spreading law.

$$\frac{dB_{eff}}{dt} = C_g \; g \sqrt{1 - \frac{\rho_a(z=0)}{\rho_m(c-c_A)}} \; H_{eff} \qquad \ldots(4.8)$$

where C_g is the spreading constant; we now use $C_g = 1.15$, following the data analysis of van Ulden (1984).

By using the definitions of H_{eff} and u_{eff}, we obtain:

$$\frac{dB_{eff}}{dx} = \frac{1}{u_{eff}} \frac{dB_{eff}}{dt} = C \sqrt{1 - \frac{\rho_a(z=0)}{\rho_m(c-c_A)}} \left(\frac{S_z}{z_o} \right)^{\frac{1}{2}-\alpha} \qquad \ldots(4.10)$$

with

$$C = C_E \frac{(gz_o)^{\frac{1}{3}}}{u_o} \left\{ \Gamma\left(\frac{1}{1+\alpha}\right) \right\}^{\frac{3}{2}} (1+\alpha)^{-\frac{1}{3}} \quad \ldots(4.11)$$

With B_{eff} determined by Equation (4.10) and S_y by Equation (4.6) the crosswind width b follows from Equation (3.13).

Above the source we neglect gravitational spreading ($B_{eff} = B$) and crosswind dispersion of the plume ($S_y = 0$; $b = B$). At some distance downwind, x_t, the half-width of the middle part of the concentration profile b becomes zero and downwind of this position the crosswind profile is completely Gaussian, with S_y given by:

$$S_y = \sqrt{2}\ \delta(x + x_v)^{\beta} \quad \ldots (4.12)$$

where x_v can be determined from $S_y(x_t) = \sqrt{2}\ \delta(x_t + x_v)^{\beta}$.

At $x = x_t$ we assume that the lateral gravitational spreading of the plume terminates.

4.2 The ground level centreline concentration c_A

Downwind of the area source the concentration c_A can be determined from the integral mass balance

$$E = \int_0^{\infty} \int_{-\infty}^{\infty} c u_x \, dy dz \quad \ldots (4.13)$$

where E is the source strength. Substituting in this expression the similarity profiles for c and u_x, equations (2.1) and (2.2), we find:

$$c_A = \frac{E(1+\alpha) z_o^{\alpha}}{2 u_o S_z^{1+\alpha} \left(b + \frac{\sqrt{\pi}}{2} S_y\right)} \quad \ldots (4.14)$$

Above the area source the ground level concentration is taken to be a constant.

Here we distinguish between two cases:

1. The vertical vapour mass flux Q_p is greater than the maximum vapour flux that can be taken up into the atmosphere, Q^*_{max}.

For a source of L_p we determine Q^*_{max} as follows: above the source we take the vapour concentration to be 100 %, i.e. $c_A = \rho_g$, the 100 % gas density at emission conditions, and define Q_{max} by:

$$Q^*_{max}\ (L_p) = \frac{\rho_g}{L_p} \int_0^{\infty} \exp \left(- \left(\frac{z}{S_z\ (x=0.5\ L_p)} \right)^{1+\alpha} \right) u_x dz = \frac{\rho_g u_o S_z^{\,1+\alpha} (x=0.5\ L_p)}{(1+\alpha) z_o^{\ \alpha} L_p} \quad \ldots (4.15)$$

This means that we neglect the crosswind gravitational spreading and the crosswind dispersion of the plume above the source, so then the problem is two-dimensional and Q^*_{max} does not depend on the width of the source. If now $Q_p > Q^*_{max}\ (L_p)$, the emitted gas cannot be directly taken up into the atmospheric wind field and a 100 % vapour blanket forms above the source. This vapour blanket is heavier than air and spreads due to gravitational forces. For the steady-state situation the gas blanket length L, half-width B, and vapour mass flux $Q = Q^*_{max}\ (L)$ must be such that the take-up rate into the atmosphere (Q).L.B. is the same as the gas production rate $Q_p.L_p.B_p$. In the steady-state model we can only deal with rectangular sources of length L_p Q^*_{max} and half-width B_p. Analogous to equation (4.15), $Q^*_{max}(L)$ can be determined from:

$$Q^*_{max}\ (L) = \frac{\rho_g u_o S_z^{\,1+\alpha} (x=0.5\ L_p)}{(1+\alpha) z_o^{\ \alpha} L} \quad \ldots (4.16)$$

and then L and B can be calculated by iteratively from the identity $Q^*_{max}(L).L.B. = Q.L_p.B_p$, assuming that $\frac{L}{L_p} = \frac{B}{B_p}$.
In the dispersion calculation we now introduce a source length L and half-width B with a ground level concentration $c_A = \rho_E$.

2. If $Q_p \leq Q^*_{max}(L_p)$, the emitted gas can be directly taken up into the atmosphere and no 100 % vapour blanket forms.

The source length L and half-width B for the dispersion calculation are now the same as the primary source length L_p and half-width B_p and the constant ground level concentration c_A above the source is determined iteratively in such a way that

$$Q = Q_p = \frac{c_A}{L_p} \int_0^{\infty} \exp -\left\{\frac{z}{S_z(x=0.5\ L_p)}\right\}^{1+\alpha} u_x dz$$

$$= \frac{c_A u_o S_z^{1+\alpha}(x=0.5\ L_p)}{(1+\alpha) z_o^{\alpha} L_p} \qquad \ldots (4.17)$$

If the source is not rectangular we treat it as a rectangular one of the same surface area.

4.3 Sources with time-dependent vapour emission rate and/or dimensions

As an example of a source with time-dependent vapour emission rate, a stationary, boiling liquefied gas pool in a diked area will be suitable. Here, as the ground cools down, the heat flux to the boiling pool decreases, resulting in a decreasing boil-off flux with time. For a spreading liquefied gas pool on land not only is the evaporation flux time-dependent but also the dimensions of the pool.

For use in the time-dependent dispersion model we assume the source to be circular with a radius $R_1(t)$, given as a function of the time

t. If the source has another shape, it is intended as a circular one of the same surface area. In addition to $R_1(t)$, the vapour production rate E(t) must be specified as a function of the time. We assume that the vertical vapour flux Q from the source is uniform over the source, so:

$$Q(t) = E(t)/(\pi R_1^2(t)) \qquad \ldots (4.18)$$

If this vertical vapour flux Q(t) is less than maximum flux that can be taken into the atmospheric flow field, Q^*_{max}, the gas is directly taken up be the wind.

The value of Q^*_{max} is calculated with the steady-state model and since we can only handle rectangular sources in the steady-state dispersion calculations, a circular source is treated as a square source of $L = \sqrt{\pi}\, R_1(t)$ and for this source length the maximum take-up flux Q^*_{max} $(L = \sqrt{\pi}\, R_1(t))$ is calculated.

If $Q(t) > Q^*_{max}$ $(L = \sqrt{\pi}\, R_1(t))$, the emitted gas cannot be directly taken up into the atmospheric wind field and a 100 % dense vapour blanket forms above the source. This gas blanket is taken to have a flat cylindrical shape of radius $R_g(t)$ and height $H_g(t)$. At the bottom of the blanket, gas is supplied from the source at a rate E(t), while from the top, gas is taken up into the wind field at a rate $\pi R_g^2(t) Q^*_{max}$ $(L = \sqrt{\pi}\, R_g(t))$, so that the mass balance for the gas blanket reads:

$$\frac{d}{dt}\left[\pi \rho_g R^2{}_g(t) H_g(t)\right] = E(t) - \pi R^2{}_g(t) Q^*_{max}(L = \sqrt{\pi} R_g(t)) \ldots (4.19)$$

It is assumed that the centre of the gas blanket remains stationary at x = 0. This assumption introduces relatively small errors, firstly because the height of the gas blanket is small and the wind velocity close to the earth's surface is low. Approximate calculations

indicate that if the blanket were to travel with the wind, the distance travelled downwind by the blanket until it had been taken up completely would be very short. Secondly, a considerable mass has to be accelerated to the wind velocity; this reducing the travelled distance even more.

Owing to the density difference with the surrounding air, the blanket will slump and spread laterally. In order to describe this gravitational spreading we use the simple spreading law

$$\frac{d\,R_s(t)}{dt} = C_E \sqrt{g\,(1 - \frac{\rho_a(z=0)}{\rho_E})\,H_s(t)} \qquad \ldots\ (4.20)$$

analogous to equation (22) describing the crosswind gravitational spreading of the plume. Given E(t) and the appropriate initial conditions we can now solve the radius $R_s(t)$ and height $H_s(t)$ of the gas blanket as functions of time. If it appears that the radius of the source $R_1(t)$ is greater than $R_s(t)$, we put $R_s(t) = R_1(t)$ and adapt the calculated value of $H_s(t)$ accordingly. Thus the radius of the gas blanket is then always equal to or greater than the radius of the source.

If a gas blanket is present, the take-up flux into the atmosphere $Q^*(t)$ is taken to be Q^*_{max} $(L = \sqrt{\pi}\,R_s(t))$, so the take-up is no longer dependent on Q(t). We therefore introduce here the concept of a secondary source of radius $R(t) = R_s(t)$ and take-up flux $Q^*(t) = Q^*_{max}$ $(L = \sqrt{\pi}\,R_s(t))$. If no gas blanket is present the take-up flux $Q^*(t)$ is Q(t) and we then define the secondary source radius to be the same as that of the real source:

$$R(t) = R_1(t)$$

Summarising, we have defined the secondary source parameters as follows:

$$R(t) = R_s(t)$$

if a gas blanket is present

$$Q^*(t) = Q^*_{max}\ (L - \sqrt{\pi}\, R_s(t))$$

and

$$R(t) = R_1(t)$$

if no gas blanket is present.

$$Q^*(t) = Q(t)$$

... (4.21)

5. THERMAL EFFECTS

The thermodynamics of the mixing of the dense gas with ambient air are calculated in a subroutine (THERMO). It is assumed that the gas, air and water vapour behave as ideal gases with constant specific heats. For cold gas releases, the condensation of water can have a significant effect, owing to the heat of condensation liberated, and there is a smaller effect from its freezing. For gases with more complex properties (such as reaction with water), a specific subroutine to calculate the special thermodynamics in that case can easily be substituted for THERMO.

One input parameter supplied to THERMO by the model is the additional heat transferred to the cloud by heat transfer. Variation of this parameter can also make allowance for varying temperatures of entrained air. It was also found necessary, for LNG releases on the sea, to allow for variation in the water content of the cloud due to vapour transfer from the surface. The modelling of these processes is described below.

5.1 Heat transfer from the surface

5.1.1 Theory

Heat transfer from the substrate to the cold vapour cloud is described by the following expressions for forced (Holman, 1981) and natural (McAdams, 1954) convection heat flux:

$$Q_{H,f} = \tfrac{1}{2} \left(\frac{\alpha_T}{\nu}\right)^{2/3} C_f \rho_m C_{pm} u (T_s - T_m) \qquad \ldots(5.1)$$

and

$$Q_{H,n} = 0.14 \left[\frac{\alpha_T^2 \zeta g}{\nu} (\rho C_p)^3 \right]^{1/3} (T_s - T_m)^{4/3} \qquad \ldots(5.2)$$

where C_f is the friction factor, u the gas velocity, T_s and T_m the temperatures of substrate and mixture and g the gravitational acceleration. The expressions contain the following gas properties: α_T the thermal diffusivity, ν the kinematic viscosity, ρ the density and C_{pm} the specific heat of the mixture. The parameter $\zeta = -\frac{1}{\rho}\left(\frac{\partial \rho}{\partial T}\right)_p$, so for an ideal gas $\zeta = 1/T$,

The friction factor $C_f = 2\left(\frac{u_*}{u}\right)^2$, where u_* is the friction velocity. For methane $\alpha_T/\nu = 1.35$; for other gases this ratio is only slightly different. For u we take the logarithmic wind velocity at 10 m height, u_{10}. Thus expression (5.1) for forced convection heat flux can be written as

$$Q_{H,f} = 1.22 \frac{u_*^2}{u_{10}} \rho C_p (T_s - T_m) \qquad \ldots(5.3)$$

For ρ, C_p and T_m we take the gas mixture properties corresponding with the ground-level centre line concentration c_A. Using the ideal gas law $p = \frac{R}{M}\rho T$, expression (5.2) for natural convection may be rewritten as:

$$Q_{H,n} = 0.14\, g^{1/3} \frac{P}{R} \left[\frac{\alpha_T^2}{\nu} \frac{\nu}{T^2} (MC_p)^3 \right]^{1/3} \left[\frac{(T_s - T_m)^2}{T} \right]^{2/3} \qquad (5.4)$$

For methane, propane and air the value of the group

$$\left[\frac{\alpha_T^2}{\nu} \frac{\nu}{T^2} (MC_p)^3 \right]^{1/3}$$

is 24, 29 and 20, respectively, in mks units.

This group is an input parameter to the model, with a default of the the methane value 24. For T in expression (5.4) we take the mean

temperature $(T_s + T_m)/2$, where T_m is the gas mixture temperature corresponding with the ground-level centre-line concentration c_A. In HEGADAS the pressure P is taken to be the standard atmospheric pressure (760 mm Hg).

The approach adopted in the calculation sequence of HEGADAS is to compute the heat fluxes for both free and forced convection. For $T_s > T_m$, the maximum value of the two is selected as the heat flux from the substrate, i.e. $Q_H = \max(Q_{H,f}, Q_{H,n})$. For $T_s < T_m$, $Q_H = Q_{H,f}$ is chosen. The heat flow picked up from the substrate can be written as $(D/V_m)\ u_{eff}\ B_{eff}\ H_{eff}$, where D is the added heat per mole of mixture and V_m is the specific molar volume of the mixture. To take heat transfer into account, the following equation is now added to the set given in Sections 3 and 4:

$$\frac{d}{dx}\left[\frac{D}{V_m}\, u_{eff}\, B_{eff}\, H_{eff}\right] = Q_H\, B_{eff}, \qquad \ldots(5.6)$$

For places where the middle part of the concentration profile has disappeared (b = 0), we take:

$$\frac{d}{dx}\left[\frac{D}{V_m}\, u_{eff}\, H_{eff}\right] = Q_H \qquad \ldots(5.7)$$

The temperature T_m and density ρ of the gas/air mixture and the specific molar volume V_m are computed in the thermodynamic subroutine for a given mole fraction of the emitted gas and a given amount of added heat D. This subroutine of the HEGADAS programme also takes into account the latent heat of condensation and of freezing of water vapour present in the air;

see Appendix A. The original formulation of vertical dispersion (equation 3.13) can be written as

$$\frac{d}{dx}\left[U_{*ff}\ B_{*ff}\ H_{*ff} \right] = ku_{*}\ (1+\alpha)\ B_{*ff}/\Phi(Ri_{*}); \qquad \ldots(5.8)$$

If the gas cloud temperature differs from ambient, relation (5.8) is not correct. For, in this case, the change in volume flow $u_{*ff}\ B_{*ff}\ H_{*ff}$ is not affected by entrainment alone, but also by changes in the specific molar volume V_m due to heat transfer from the substrate and mixing with air of a different temperature. These effects have been taken into account by formulating the entrainment relation in terms of mole flow:

$$\frac{d}{dx}\left[u_{*ff}\ B_{*ff}\ H_{*ff}/V_m \right] = ku_{*}\ (1+\alpha)\ B_{*ff}/(V_o\Phi(Ri_{*})) \qquad \ldots(5.9)$$

with V_o the molar volume of air. If the constant middle part of the concentration profile has disappeared (b = 0), we now use:

$$\frac{d}{dx}\left[u_{*ff}\ H_{*ff}/V_m \right] = ku_{*}\ (1+\alpha)/(V_o\ \Phi(Ri_{*})). \qquad \ldots(5.10)$$

5.1.2 Experimental test

In order to study the processes of heat transfer, water vapour transfer and convective entrainment in dense gas clouds, a series of laboratory experiments involving cold nitrogen flowing across a water surface were conducted. These are described by Colenbrander and Puttock (1984) and in Appendix 1. The results of series 3 of the experiments (heat

transfer without water vapour transfer) were used to test this heat transfer relation.

The natural convection heat flux is calculated for the conditions at the middle of the box (location B) during the series 3 experiment. For the vapour temperature we found T_g = 161.4 K and for the oil surface temperature we take T_s = 286 K.

Hence we find

$$Q_{H,n} = 75 \times 16.9 \text{ Wm}^{-2} = 1270 \text{ Wm}^{-2} \qquad (5.11)$$

The forced convection heat flux was calculated with equation (5.1), using α_T/ν = 1.35 and C_f = 0.005. For u in equation (5.1) we took the bulk velocity of the vapour stream, which was calculated from the nitrogen flow rate and the estimated height of the vapour stream as outlined below.

The nitrogen release rate was taken to be 83 kg/h, i.e. the rate at 700s from the start of the release. At a temperature of 161.4 K we find a density of 2.1 kg/m^3 and hence a volume flow rate of 0.011 m^3/s. From the temperature profiles we determined the height of the vapour stream to be 0.06 m. Since the width of the box was 1 m we then arrived at a bulk velocity u = 0.18 m/s. Equation (5.1) then gives $Q_{H,f}$ = 150 Wm^{-2} which is almost an order of magnitude smaller than the calculated free convection heat flux.

The calculated free convection heat flux $Q_{H,n}$ = 1270 Wm^{-2} is some 20% lower than the heat flux, calculated from the measured temperature increase.

We also used HEGADAS to calculate the temperature increase between location A and C. As gas emission temperature we took 140.6 K, the measured temperature at location A. The nitrogen release rate was 83 kg/h. The "wind velocity" was taken to be 0.18 m/s at a reference

height of 0.01 m. The roughness length was chosen to be 10^{-5}, giving $u_* = 0.01$ m/s. The gravitational spreading and dispersion in the crosswind direction were set to zero and the plume width was taken constant.

Figure 6 shows the HEGADAS calculation of the heat transfer rate, compared with observations. The calculation gives an air concentration increase of 1.3% per 0.5 m, in agreement with the experimental findings. Air entrainment is further discussed in Section 5.3.

5.2 Transfer of water vapour from a water surface into the cloud

The mechanism by which condensation within the thermal boundary layer can increase the rate of evaporation from a liquid surface has been described by Turkdogan (1964) and Rosner (1967). In the following, we take the theoretical approach of Rosner (1967).

Figure 7 shows schematically vapour pressure profiles immediately above the surface of a liquid evaporating into a colder gas. It is assumed (and confirmed *a postiori*) that the condensation does not significantly change the temperature profile across the boundary layer. Curve A shows the vapour pressure profile in the absence of any condensation. If there were condensed water present at all levels in the boundary layer, then the vapour pressure profile would be curve B, which is the equilibrium vapour pressure corresponding to the local temperature at each level. In fact, provided foreign nuclei are not available in this region, condensation cannot begin until the vapour pressure reaches critical supersaturation s_{crit}, which is again a function of the local temperature, and is indicated as curve C. The actual vapour pressure profile, therefore, must intersect curve C. It can be shown that the stable solution is the one in which the profile is tangential to curve C, i.e. curve D.

Rosner presents solutions of the transcendental equation for the dimensionless form Δ of the reduced boundary layer thickness δ_n, where

$$\Delta = \frac{\delta_n}{T_s}\left[-\frac{\partial T}{\partial z}\right]_{z=0}, \qquad \delta_n = p_{wv}(0) \Big/ \left[-\frac{\partial p_{wv}}{\partial z}\right]_{z=0} \qquad (5.12)$$

Δ is a function of three dimensionless parameters

$$\mathcal{N} = \frac{N}{R\,T_s}, \text{ where } \quad N = R\left[\frac{d(\ln s_{crit})}{d(1/T)}\right]_{T=T_s} \approx \text{const.}, \qquad (5.13)$$

$$\mathcal{L} = \frac{c_p}{R\,T_s}, \qquad \mathcal{D} = s_{crit}(T_s).$$

For water, N/R is approximately 1200 K (Derived from data in Figure 7-4 of Pruppacher and Klett, 1978). With the use also of values of $\mathcal{L}$ and $\mathcal{D}$ appropriate to water, Rosner's plotted results then give values of Δ which are in the range 0.20 ± 0.01 for $0°C \le T_s \le 30°C$. We therefore use the value 0.20 for Δ.

The water vapour flux from the surface is then

$$Q_{wv} = \frac{1}{\Delta}\,\frac{(p_{wv}(T_s) - p_{wv}(T_m))}{C_{pm}\,T_s\,p}\,Q_H \qquad \ldots(5.14)$$

In this expression we substitute for Q_H the heat flux calculated as described in section 5.1. For C_{pm} we take the gas mixture properties corresponding with the ground-level centre line concentration C_A.

The transfer of water vapour from the surface is then taken into account in HEGADAS by adding a further differential equation:

$$\frac{d}{dx}\left[y_{w3}\ u_{eff}\ B_{eff}\ H_{eff}/V_m \right] = Q_{wv}\ B_{eff}$$

or

$$\frac{d}{dx}\left[y_{w3}\ u_{eff}\ H_{eff}/V_m \right] = Q_{wv} \qquad \ldots(5.15)$$

if the middle part of the concentration profile has disappeared (b = 0). In these expressions y_{w3} is the molar fraction of picked-up water vapour in the cloud.

The picked-up water vapour also contributes to the total molar flow in the cloud and we therefore extend the entrainment relations (5.9) and (5.10) to, respectively.

$$\frac{d}{dx}\left[u_{eff}\ B_{eff}\ H_{eff}/V_m \right] = \left[ku_* \ (1 + \alpha)\ /(V_o\ \Phi(Ri_*)) + Q_{wv} \right] B_{eff} \qquad (5.16)$$

and, if b=0,

$$\frac{d}{dx}\left[u_{eff}\ H_{eff}/V_m \right] = ku_* \ (1 + \alpha)\ /(V_o\ \Phi(Ri_*)) + Q_{wv} \qquad (5.17)$$

Solution of the set of differential equations by HEGADAS gives y_{w3} as a function of downwind distance x. Given y_{w3}, the thermal effects of the picked-up water vapour are taken into account in the thermodynamic subroutine.

The predictions of this model can be tested against the nitrogen-box experiments. In Figure 8, the observations of the increase in water content between locations A and C in the series 2 experiments are shown. The predictions of HEGADAS are in good agreement with these

observations. In Figure 9, the predicted temperature increase with distance for the series 2 experiments is plotted together with the experimental data. Incorporation of water vapour pick-up gives very good agreement.

5.3 Convective entrainment

The objective of the laboratory experiments described in Appendix 1 was to study air entrainment caused by convective advents due to the temperature difference between the substrate and a cold vapour cloud.

To characterise the turbulence in a free convection layer a velocity scale w_* has been defined

$$w_* = \left[\frac{g\, Q_H\, H_{eff}}{T_m\, \rho_m\, C_{pm}} \right]^{1/3} \qquad \ldots(5.18)$$

where H_{eff} is the layer height.

We estimated the heat flux Q_H at location B in the series 3 experiments to be 1.6 kW/m^2. The height of the vapour stream for these experiments was found to be 0.06 m and M C_p = 29.3 kJ/kmole for nitrogen vapour. Using the numerical values of g, R and the atmospheric pressure p, we find w_* = 0.14 m/s. This value is an order of magnitude larger than the estimated value for u_*: 0.01 m/s.

Several proposals have been made for model formulations to describe convective entrainment (Eidsvik, 1980; Zeman, 1982; Jensen and Mikkelsen, 1984). We follow the simple approach of Eidsvik by taking

$$u_T = u_*^2 + (a\, w_*)^2 \qquad \ldots(5.19)$$

as the velocity scale determining the turbulent entrainment rate. The constant a is determined experimentally as shown below. The full

mathematical representation of vertical entrainment in HEGADAS is now obtained by replacing u_* with u_T in relation (5.16)

$$\frac{d}{dx}\left[u_{*ff}\ B_{*ff}\ H_{*ff}/V_m\right] = \left[ku_T\ (1+\alpha)/(V_o\ \Phi(Ri_*)) + Q_{wv}\right] B_{*ff} \qquad (5.20)$$

wherby Ri_* is given by equation (3.6) with u_* replaced by u_T.

After incorporation of the model formulation for convective entrainment HEGADAS calculations were done for the conditions during the series 2 experiments. The value of the constant a was chosen to fit the experimental data on air entrainment. Good agreement was obtained for a = 0.2 (Figure 10) so

$$u_T = u_*^2 + (0.2\ w_*)^2 \qquad \ldots(5.21)$$

6. THE TIME-DEPENDENT MODEL

The formulation described above provides the steady state version of the HEGADAS model. The time-dependent version of the model is capable of dealing with arbitrary time variation of the release rate of gas at the source, such as might be derived from an evaporating liquid pool.

6.1 The transient dispersion model

In order to visualise the quasi-steady-state description of the transient behaviour of dense vapour clouds, we will follow observer "i", one of a number of observers travelling at a regular time interval Δt over the source. The subscript i refers to quantities associated with observer i.

The velocity $u_i(t)$ of observer i is time-dependent; the way in which it is related to the wind velocity u_x is described in Appendix B. The observer velocity increases with downwind distance and for all observers their velocity at a given location x is the same ($u_i(x = u_{i+1}(x))$. This implies that at a given time t the velocity of observer i is greater than the velocity of the following observer ($u_i(t) > u_{i+1}(t)$).

Let observer i encounter the upwind edge of the secondary source at $t = t_{1i}$ and the downwind edge at $t = t_{2i}$ (see Fig. 11) and let $x_i(t)$ be the location of this observer at time t. As can be seen from Fig. 11 the local secondary half-width of the source $B_i'(t)$ observed at time t is given by:

$$B_i'(t) = \sqrt{R^2(t) - x_i^2(t)} \qquad \ldots (6.1)$$

The secondary source area A_i seen by observer i is found by evaluating the integral

$$A_i = \int_{t_{1i}}^{t_{2i}} u_i(t)\, B_i'(t)\, dt \qquad \ldots (6.2)$$

The secondary source length L_i as seen by observer i is given by:

$$L_i = x_i(t_{2i}) - x_i(t_{1i}) \qquad \ldots (6.3)$$

and thus we find an average observed secondary half-width of the source

$$B_i = A_i/L_i \qquad \ldots (6.4)$$

Similarly, the average take-up flux Q_i^* of observer i may be found from:

$$Q_i^*\, B_i L_i = \int_{t_{1i}}^{t_{2i}} Q^*(t) B_i'(t) u_i(t) dt \qquad \ldots (6.5)$$

In this way we can determine, for each of the n observers travelling over the source (i = 1,n), the observed dimensions L_i and B_i, the locations $x_i(t_{1i})$ and $x_i(t_{2i})$ of, respectively, the upwind and the downwind edge of the secondary source and the average take-up flux Q_i^*. From these concentration distribution in the cloud can be determined at a specified time t_s.

To this end the location $x_i(t_s)$ of each observer at time t_s is calculated and for each observer a steady-state calculation is done, using the pertinent parameters L_i, B_i Q_i^* and $x_i(t_{2i})$. Thus the concentration distribution parameters $c_A(x_i(t_s))$, $S_y(x_i(t_s))$, $b(x_i(t_s))$, $S_z(x_i(t_s))$ are determined for i = 1,n and thus the concentration distribution $c(x_i(t_s),y,z)$, given by equation (2.1).

It will be clear that in this quasi-steady state approach the gravitational spreading of the cloud in the wind direction cannot be taken into account, unlike in heavier gas dispersion model for strictly instantaneous vapour releases, see Cox and Roe (1977) and Germeles and Drake (1975). Thus, the width of the cloud calculated with the model presented here will be somewhat too large and the length too small, especially at very low wind velocities. In the calculated concentration levels in the bulk of the cloud we only introduce second order errors with this approach. We consider the alternative, a model for an instantaneous release, as being less attractive, since a spill will only occasionally result in a strictly instantaneous vapour release. Some spreading in the wind direction is introduced in the gas blanket calculation, where we can use a radial spreading law because the centre of the gas blanket is assumed to remain stationary above the source at $x = 0$. In addition, a correction algorithm has been devised for use at the end of the calculation, which redistributes part of the lateral gravity spread to longitudinal spreading (see Appendix C). An input parameter determines whether this correction is applied.

For releases of short duration, dispersion in the wind direction may have a significant influence on the concentration level in the cloud. Accordingly, the calculated concentrations are adjusted to take account of this dispersion in the x-direction. The method followed is described in the next section.

6.2 Dispersion in the wind direction

Experiments have shown that the ground level gas concentration distribution due to an instantaneous release of e kg/m^2 tracer gas from an

infinite crosswind plane source at x = 0 can be reasonably well described by:

$$c(x;x_o) = \frac{e}{\sigma_x(x_o)\sqrt{2\pi}} \exp -\left\{\frac{(x - x_o)^2}{2S_x^2(x_o)}\right\} \quad \ldots (6.6)$$

In this expression x_o represents the location of the centre of gravity of the puff and is a function of the time elapsed since the release because the puff travels with the wind.

Literature data on σ_x as function of the downwind distance are scarce and not very well established see Beals (1971), Davies and Shair (1974), Suffman (1962), Tyldesley and Willington (1965) and Chatwin (1968). These data have been partly obtained from theoretical considerations and partly from experiments. On the basis of these data we have taken

$$S_x(x_o) = a_x x^{b_x} \quad \ldots (6.7)$$

for all atmospheric stability classes.

Let $c_A(x)$ be the ground level axis concentration of the plume, calculated as described earlier. We consider this concentration distribution as being due to the release of successive puffs of varying quantity $c_A(x_p)$ dx without dispersion in the x direction (see Fig. 12). Analogous to equation (40), the dispersion in the x-direction is taken into account by replacing an element of the concentration distribution of height $c_A(x_p)$ and width dx by an element with a Gaussian distribution

$$c'_A(x;x_p) = \frac{c_A(x_p)dx}{\sigma_x(x_p)\sqrt{2\pi}} \exp -\left\{\frac{(x - x_p)^2}{2\sigma_x^2(x_p)}\right\} \quad \ldots (6.8)$$

having the same area $c_A(x_p)dx$ (see Fig. 3).

The concentration distribution, corrected for dispersion in the x-direction, $c'_A(x)$ is then found by adding up the contributions to the concentration at point x of all he Gaussian distributed elements:

$$c'_A(x) = \frac{1}{\sqrt{2\pi}} \int_0^{\infty} \frac{C_A(\xi)}{\sigma_x(\xi)} \exp\left\{-\frac{(x-\xi)^2}{2\sigma_x^2(\xi)}\right\} d\xi \qquad \ldots (6.9)$$

The only variable in the spatial concentration distribution, equation (2), which is corrected for this dispersion is the cloud axis concentration c_A. Even in a non-instantaneously released, but neutrally buoyant cloud, this correction would not be strictly rigorous for locations off the cloud axis since the variables S_y, b and S_z depend on the x-location in the cloud. This applies the more to a heavy gas cloud where the growth of S_y, b and S_z with the downwind distance x depends on the local gas concentration. It does not seem possible, however, to apply a more rigorous correction for dispersion in the x-direction without moving away from the basic concepts of the discussed model.

6.3 Solution of the equations

The equations describing the time-dependent heavy gas dispersion problem given in the preceding sections are solved in a computer program written in Fortran 77. As input for this dispersion program, HEGADAS (heavy gas dispersion from area sources), the vapour production rate and source radius have to be given as functions of time. In addition, HEGADAS requires the atmospheric flow field parameters ρ_a $(z = 0)$, u_o, z_o, z_R, λ, the point source dispersion parameters δ and β, the spreading constant C_E and the gas density ρ_E.

The program calculates the value of α and the dispersion parameters $c_A(x)$, $S_z(x)$, $S_y(x)$ and b(x) at fixed distance intervals Δx and

at specified times. Then the spatial concentration distribution at a specified time is given by relation (2). The program also evaluates the coordinates of concentration isopleths in the $y = 0$ and $z = 0$ planes at a given time for two specified concentration values c_U and c_L. Further, it calculates the vapour mass and the volume of those parts of the cloud where the concentration is $\geq c_L$ and $\geq c_U$. The latter feature enables us to determine, for example, the cloud content between the flammability limits c_{UFL} and the iso-concentration contours for these concentration levels at specified times in the case of a flammable gas release.

6.4 Instantaneous gas release

For an instantaneous release of gas, or in very low winds, gravity spreading of the cloud in all directions, rather than just laterally, is important. For these circumstances, the model "HEGABOX" has been developed which treats the cloud as an expanding cylinder in its early stages (Puttock, 1988a). It has a smooth transition into HEGADAS for calculation of the dispersion further downwind, if required.

7. COMPARISON WITH EXPERIMENT

In the development of the model, the empirical input has been derived from laboratory experiments which, as far as possible, isolate the various physical mechanisms being considered. Comparison of model predictions with field data are then a validation of the model, rather than "calibration". (In the case of water vapour transfer, initial comparison showed that a significant mechanism was missing from the model, which was subsequently quantified in laboratory experiments.) The principal source of data for the validation of HEGADAS in the steady state has been the series of liquefied gas releases at Maplin Sands. These included steady releases of propane and LNG. The LNG plumes were affected significantly by surface heat transfer and water vapour transfer; indeed, the need to take water vapour transfer into account was deduced from analysis of the LNG experiments. For propane, however, these additional effects were not significant. Results of the comparison of predictions by HEGADAS and the field observations are given in a series of papers (Puttock et al., 1982, 1984, Colenbrander and Puttock, 1984). Good overall agreement is obtained for propane releases ,and equally satisfactory agreement is obtained for LNG provided both surface heat transfer and water vapour transfer are taken into account.

Comparisons of HEGABOX/HEGADAS predictions with observations at Thorney Island are given by Puttock (1987).

8. CONCLUSIONS

1. An integral model for the dispersion of an initially dense gas has been formulated, using similarity profiles for the concentration in the vertical and crosswind directions.
2. Vertical mixing is based on wind tunnel and water channel experiments. It appears that practical calculations are unlikely to be affected by the form of the entrainment relation beyond the limits of the wind tunnel data, which have the most direct relevance to atmospheric dispersion.
3. The cloud spreads laterally owing to gravity, and also the edges diffuse. Atmospheric correlations for the lateral dispersion coefficient S_y are extended to infer the development of a profile with a uniform mid-part and diffuse edges.
4. Laboratory experiments with a layer of cold nitrogen flowing over water have confirmed the adequacy of three aspects of the model: (a) standard free-convection heat transfer at low velocities, (b) a formulation for water vapour transfer based on the critical supersaturation approximation for condensation within the thermal boundary layer, and (c) a convective entrainment formulation.
5. Comparison of model predictions against field data, presented in other papers, shows good agreement with observations, and demonstrates, for LNG releases on the sea, the necessity of taking into account both heat transfer and water vapour transfer to the gas clouds.

REFERENCES

Beals, G.A. (197I) Guide to local diffusion of air pollutants, Techn. report 214 Air Weather Service USAF, NTIS:AD 726984.

Britter, R.E. (1980), Personal communication. See Britter (1988).

Britter, R.E. (1988), A review of mixing experiments relevant to dense gas dispersion. In: Stably Stratified Flow and Dense Gas Dispersion, (J.S. Puttock, ed.), Oxford Univ. Press.

Businger, J.A. (1973), in "Workshop on Micrometeorology", ed. D.A. Haugen, American Meteorological Society, Boston, Mass.

Chatwin, P.C. (1968) The dispersion of a puff of passive contaminant in the constant stress region, Quart. J.R. Met. Soc., 94, 350-360.

Colenbrander, G.W. (1980), "A mathematical model for the transient behaviour of dense vapour clouds", 3rd. Intl. Symp. on Loss Prevention and Safety Promotion in the Process Industries, Basle.

Colenbrander, G.W. and Puttock, J.S. (1984), Maplin Sands experiments 1980: interpretation and modelling of liquefied gas spills on the sea. In "Atmospheric Dispersion of Heavy Gases and Small Particles". (G. Ooms and H. Tennekes, eds.), Springer-Verlag, Berlin.

Cox, R.A. and Roe, D.R. (1977) A model of the dispersion of dense vapour clouds. 2nd. Int. Symp. on Loss Prevention and Safety Promotion in the Process Industries, Heidelburg.

Deardorff, J.W. and Willis, G.E. (1982) "Dependence of mixed-layer entrainment on shear stress and velocity jump", J. Fluid Mech., 115, 123-149.

Drivas, P.J. and Shair, F.H. (1974) Dispersion of an instantaneous crosswind line of tracer release from an urban highway, Atm. Env., 8 , 475-485.

Eidsvik, K.J. (1980) "A model for heavy gas dispersion in the atmosphere", Atmos. Eviron., 14, 769-777.

Ellison, T.H. and Turner, J.S. (1959), Turbulent entrainment in stratified flows, J. Fluid Mech., 6, 423-448.

Germeles, A.E. and Drake, E.M. (1975) "Gravity spreading and atmospheric dispersion of LNG vapour clouds". 4th Int. Symp. on the Transport of Hazardous Cargoes by Sea and Inland Waterways", Jacksonville.

Holman, J.I. (1981), Heat Transfer, 5th ed., McGraw-Hill.

Horst, T.W. (1979), Lagrangian similarity modelling of vertical diffusion from a ground-level source, J.Appl. Met., 18, 733-740.

Jensen, N.O. and Mikkelsen, T. (1984) "Entrainment through the top of a heavy gas cloud, numerical treatment", in "Air Pollution modelling and its Application III", (ed. C. de Wispelaere) Plenum Press, New York.

Kantha, L.H., Phillips, O.M. and Azad, R.S. (1977) On turbulent entrainment at a stable density interface, J. Fluid Mech., 79, 753-768.

Kato, H. and Phillips, O.M. (1969), On the penetration of a turbulent layer into stratified fluid, J. Fluid Mech., 37, 643-655.

Kranenburg, C. (1984) "Wind-induced entrainment in a stably stratified fluid", J. Fluid Mech. 145, 253-273.

Lofquist, K. (1960) "Flow and stress near an interface between stratified liquids", Physics of Fluids, 3, 158-175.

Lowe, P.R. and Ficke, J.M. (1974) Techn. Paper No. 4-74, Environmental prediction research facility, Naval Post Grad. School, Monterey, Calif. (or see Pruppacher and Klett, 1978).

McAdams, W.H. (1954) "Heat Transmission", (McGraw-Hill).

McQuaid, J. (1976), "Some experiments on the structure of stably-stratified shear flows", Technical Paper p.21 Safety in Mines Research Establishment Sheffield U.K.

Moore, M.J. and Long, R.R. (1977), "An experimental investigation of turbulent stratified shearing flow", J. Fluid Mech., 49, 635-655.

Price, J.F. (1979) "On the scaling of stress-driven entrainment experiments", J. Fluid Mech., 90, 509-529.

Pruppacher, H.R. and Klett, J.D. (1978) Microphysics of Clouds and Precipitation. (D. Reidel, Dordrecht).

Puttock, J.S., Colenbrander, G.W. and Blackmore, D.R. (1982) Maplin Sands experiments 1980: dispersion results from continuous releases of refrigerated liquid propane. Heavy Gas and Risk Assessment II (S. Hartwig, ed.) D. Reidel, Dordrecht, 147-161.

Puttock, J.S., Colenbrander, G.W. and Blackmore, D.R. (1982) Maplin Sands experiments 1980: dispersion results from continuous releases of refrigerated liquid propane and LNG. Air Pollution Modelling and its Application (C. de Wispelaere, ed.) Plenum, New York, 353-373.

Puttock, J.S. (1987) Comparison of Throney Island data with predictions of HEGABOX/HEGADAS. J. Hazardous Materials, 16,439-455.

Puttock, J.S. (1988) A model for gravity-dominated dispersion of dense gas clouds. In: Stably Stratified Flow and Dense Gas Dispersion (J.S. Puttock, ed.) Oxford Univ. Press.

Rosner, D.E. (1967) Enhancement of diffusion-limited vaporization rates by condensation within the thermal boundary layer. I.The critical supersaturation approximation. Int. J. Heat Mass Transfer, 10, 1267-1279.

Saffman, P.G. (1962) The effect of wind shear on horizontal spread from an instantaneous ground source, Quart. J.R. Met. Soc., 88, 382.

Scanton, D.R. and Lindberg, W.R. (1983) "An experimental study of entraining, stress-driven, stratified flow in an annulus", Phys. Fluids, 26, 1198-1205.

te Riele, P.H.M., (1977) "Atmospheric dispersion of heavy gases emitted at or near ground level". 2nd. Int. Symp. on Loss Prevention and Safety Promotion in the Process Industries, Heidelberg.

Thompson, R.O.R.Y., "A reinterpretation of the entrainment process in some laboratory experiments", Dyn. Atmos. Oceans, 4, 45-55.

Turkdogan, E.T. (1964), The theory of enhancement of diffusion-limited vaporization rates by a convection-condensation process. Part I - Theoretical. Trans. Metall. Soc. AIME, 230, 740-753.

Turner, J.S. (1968) The influence of molecular diffusivity on turbulent entrainment across a density interface. J. Fluid Mech., 33, 639-656.

Turner, D.B. (1969) Workbook of atmospheric dispersion estimates. U.S. Dept. of Health, Education and Welfare. Public Health Service Publication no. 999-AP-26.

Tyldesley, J.B. and Wallington, C.E. (1965) The effect of wind shear and vertical diffusion on horizontal dispersion, Quart. J.R. Met. Soc., 91, 158-174.

van Ulden, A.P., (1984), A new bulk model for dense gas dispersion: two-dimensional spread in still air. In: Atmospheric Dispersion of Heavy Gases and Small Particles, (G. Ooms and H. Tennekes, eds.) pp.419-440 Springer-Verlag, Berlin.

Zeman, O. (1982), "The dynamics and modelling of heavier-than-air cold gas releases", Atmos. Environ., 16, 741-751.

APPENDIX A

The thermodynamics of a mixture of evaporating liquefied gas, moist air and entrained water. Calculation of temperature and density in subroutine THERMO

A.1 Introduction

This appendix details the thermodynamic equations needed for calculating the temperature and density of a cloud of cold hydrocarbon gas, mixed in arbitrary proportions with ambient air with the possible inclusion of evaporating droplets of liquefied gas and of water picked up from the sea surface. The equations form the basis of subroutine THERMO. Figure 13 indicates the dependence of various quantities on others and so the necessary sequence of calculations.

A.2 Notation

y_{wg}	molar ratio: wet gas/total mixture
ω_1'	molar ratio: water initially in air/dry air
ω_2'	molar ratio: water initially in gas ("picked up")/gas
y	molar proportions: $y_g + y_a + y_w = 1$ $y_{w1} + y_{w2} = y_{wv} + y_{wn} = y_w$
r_h	relative humidity in atmosphere
P_v	water vapour pressure
P	atmospheric pressure (in current HEGADAS version $P = P_{st}$)
P_{st}	standard atmospheric pressure 760 mm Hg

M	molecular weight (kg/kmol)
c_p	specific heat (molar)
h_{gv}, h_{wv}, h_{wf}	heat of vaporisation of gas, water; heat of fusion of water at 0°C (all molar)
T, T'	temperature in K, °C $T = T' + 273.15$
T_{st}	standard temperature: 273.15°K
ρ	density
	density ratio of air at same temperature
V	molar volume
V_o	molar volume at s.t.p., 0.0224 m^3
D	heat transferred from surface per mole of mixture
n	moles

Subscripts

g	gas (hydrocarbon)
gv, gl	gas in vapour phase, liquid gas
gl0	gas as liquid aerosol at time t = 0 (in the current HEGADAS version no aerosol is allowed)
a	air (dry)
w	water
w1, w2	water initially in air, gas
w3	water from surface
wv, wl, wi	water vapour, liquid water, ice
wn	non-vapour water (liquid or solid)
m	mixture (i.e. total cloud)

A.3 Thermodynamic equations

The molar proportions of the various components in the mixture can be calculated from their definitions and the definition of the vapour pressure of water:

$$\omega_1' = \frac{r_h P_v(T_a)/P}{1 - r_h P_v(T_a)/P} \qquad \ldots (A.1)$$

$$y_g = \frac{y_{wg}}{1 + \omega_2'} \qquad y_a = \frac{1 - y_{wg} - y_{w3}}{1 + \omega_1'}$$

$$\ldots (A.2)$$

$$y_{w2} \frac{w_{wg}\omega_2'}{1 + \omega_2'} \qquad y_{w1} = \frac{(1\ y_{wg} - y_{w3})\omega_1'}{1 + \omega_1'}$$

$$y_{wv} = \min \left\{ \frac{(y_g + y_a)\ P_v\ (T_m)/P}{1 - P_v\ (T_m)/P},\ y_w \right\} \qquad \ldots (A.3)$$

$$y_{wn} = y_w - y_{wv} \qquad \ldots (A.4)$$

An empirical expression for the vapour pressure of water $P_y(T)$ is given below. Since the temperature of the mixture is initially unknown, the temperature at the previous time step should be used in (A.3). The estimate is improved by iteration.

The mixture temperature is calculated by evaluating the enthalpy of each component of the mixture before and after mixing and equating the initial and final total enthalpies. In all cases enthalpy will be taken to be zero at 0°C in the gaseous state. Specific heats will be assumed to be independent of temperature. (The specific heat of methane in fact varies by ±2% from its mean between -161°C and 20°C.)

Enthalpy of air initially $= n_m\, y_a\, T'_a\, c^*_{pa}$

finally $= n_m\, y_a\, T'_m\, c^*_{pa}$ ... (A.5)

Enthalpy of water initially $= n_m\, y_{w1}\, T'_a\, c^*_{pwv}$

$+ n_m\, y_{w2}\, (T'_{w2}\, c^*_{pwl} - h^*_{wv})$ ... (A.6)

finally $=$

$$\begin{cases} n_m\, y_{wv}\, T'_m\, c^*_{pwv} + n_m\, y_{wn}\, (T'_m\, c^*_{pwl} - h^*_{wv}) & \text{for } T'_m > 0 \\ n_m\, y_{wv}\, T'_m\, c^*_{pwv} + n_m\, y_{wn}\, (T'_m\, c^*_{pwi} - h^*_{wv} - h^*_{wf}) & \text{for } T'_m < 0 \end{cases}$$

Here it is assumed that the non-vapour water is ice when the temperature is below 0°C. Supercooled water should not be found since the initial temperature of the cloud (for LNG) is low enough to ensure ice nucleation.

Enthalpy of gas initially $= n_m\, y_g\, T'_g\, c^*_{pg} - n_m (y_{glo}/y_{go}) y_g\, h^*_{gv}$ ... (A.7)

finally $= n_m\, y_g\, T'_m\, c^*_{pg}$

assuming that all the gas has evaporated in the final state.

The term between brackets is (A.7) denotes the molar ratio of initial liquid gas to initial dry gas; in the present HEGADAS version this ratio is taken to be zero.

Heat transferred from sea surface = n_m D ... (A.8)

Equating total enthalpy before and after mixing gives:

$$T_m' = (y_a T_a' c^*_{pa} + y_{w1} T_a' c^*_{pwv} + y_{w2} T_{w2}' c^*_{pwl}$$

$$+ (y_{wn} - y_{w2}) h_{wv} + \underline{y_{wn} h_{wf}} + y_g T_g' c_{pg}$$

$$- y_{glo} h_{gv} + D)$$

$$\bullet$$

$$+ (y_a c_{pa} + y_{wv} c_{pwv} + y_{wn} c_{pwl} + y_g c_{pg}) \quad \ldots (A.9)$$

Equation (A.9) is only correct if T_m' is less than 0°C. Otherwise the underlined terms should be changed: the first to zero, and the second to $y_{wn} c^*_{pwl}$. In computation it will be necessary to try both forms, and if one is self-consistent then that is correct. If assuming $T_m' < 0$ gives a result > 0 and vice-versa, then the ice is partially melted and $T_m' = 0$.

If all the liquid gas has not evaporated in the final state then equation (A.8) is wrong. A proper treatment for the presence of unevaporated liquefied gas requires a knowledge of the vapour pressure as a function of temperature, since under the equilibrium conditions the temperature will fall below T_g' until the vapour pressure is equal to the partial pressure of the gas in the gas-air mixture. In the absence of vapour pressure data, the subroutine takes the simplistic assumption that the temperature does not fall below T_g'. (Note that currently the optior to specify part of the gas as liquid aerosol, $w_{glo} < 0$, is not provided i.. HEGADAS.) When the temperature is set at the boiling point of the liquid

gas T_g', equation (A.9) can be inverted to determine how much liquid gas has vaporised:

$$y_{g1o} - y_{g1} = (y_a c^*_{pa} (T_a' - T_g') + (y_{w1} T_a' - y_{wv} T_g') c^*_{pwv}$$

$$+ y_{w2} T_{w2}' \; c^*_{pw1} - y_{wn} T_g' c^*_{pwi} \qquad \ldots (A.10)$$

$$+ (y_{wn} - y_{w2}) h^*_{wv} + y_{wn} h^*_{wf} + h^*_a)/h^*_{gv}$$

The ratio of the density of the mixture to that of (moist) air at the same temperature is:

$$\rho_o/\rho_{aw} = \frac{(y_g M_g + y_a M_a + y_w M_w)(1 + \omega_1')}{(y_{gv} + y_a + y_{wv})(M_a + \omega_1' M_w)} \qquad \ldots (A.11)$$

assuming that the liquid is in a aerosol small enough to move with the gas and so contribute to the dynamics of the cloud, but has negligible volume. The actual density of the mixture is then given by:

$$\rho_m/\rho_{aw} = \frac{\rho_o}{\rho_{aw}} \Big/ \frac{T_m}{T_a} \qquad \ldots (A.12)$$

and the molar volume by:

$$\frac{V_m}{V_o} = (y_{gv} + y_a + y_{wv}) \frac{T_m}{T_{st}} \frac{P_{st}}{P} \qquad \ldots (A.13)$$

A.4 Empirical function for water vapour pressure

For temperatures from 0°C to 50°C the vapour pressure of water $P_v(T)$ can be calculated, in bars, for T' in degrees C, from Lowe and Ficke:[27]

$$P_v = a_o + T'\,(a_1 + T'(a_2 + T'(a_3 + T'(a_4 + T'(a_5 + a_6 T'))))))$$

where $a_o = 6.1078$
$a_1 = 4.4365 \times 10^{-1}$
$a_2 = 1.4289 \times 10^{-2}$
$a_3 = 2.6506 \times 10^{-4}$
$a_4 = 3.0312 \times 10^{-6}$
$a_5 = 2.0341 \times 10^{-8}$
$a_6 = 6.1368 \times 10^{-11}$

Below 0°C, the following is adequate for the vapour pressure of ice:

$$P_v(T) = b_1 \exp(-b_2/T)$$

where $b_1 = 2.624 \times 10^{10}$, mmHg $= 3.498 \times 10^{7}$ bars
$b_2 = 6134$ K

APPENDIX B

Wind velocity and observer velocity

B.1 The wind velocity profile

The best way of describing the wind velocity in the atmosphere surface layer[9] is:

$$u_x(z) = \frac{u_*}{k}\left[\ln\left(\frac{z + z_R}{z_r}\right) - \Psi_1\left(\frac{z}{\lambda}\right)\right] \qquad \ldots (B.1)$$

where

$$\Psi_1(z/\lambda) = -4.7\, z/\lambda \qquad \text{for } 1/\lambda > 0 \text{ (stable atmosphere)} \qquad \ldots (B.2)$$

and

$$\Psi_1(z/\lambda) = 2\ln\left[(1+a)/2\right] + \ln\left[(1+a^2)/2\right] - 2\tan^{-1}(a) + \pi/2 \text{ for } 1/\lambda < 0 \qquad \text{(unstable atmosphere)} \qquad \ldots (B.3)$$

with $a = (1 - 15\, z/\lambda)^{\frac{1}{4}}$ $\qquad \ldots (B.4)$

However, to be consistent with the similarity profiles for the concentration, equation (2), we have to use a wind velocity profile of the form

$$u_z = u_o\left(\frac{z}{z_o}\right)^{\alpha} \quad \text{(equation (2.2).}$$

The value of α is determined from the best fit with expression (B.1). Expression (B.1) is used directly in calculating u_* for given $u_x(z=z_o)=u_o$; the value of u_* is used in the differential equation for S_z (equation (3.4)) and in calculating the value of Ri_* (equation (3.6)).

B.2 Relation of observer velocity u_x to wind velocity u_z

The observers are released from the point $x = -R_{max}$, where R_{max} is the maximum radius of the secondary source R(t). The average transport velocity of the vapour molecules for given S_z is expressed by relation (3.10):

$$u_{eff} = u_o \left(\frac{S_z}{z_o}\right)^{\alpha} \frac{1}{\Gamma\left(\frac{1}{1+\alpha}\right)} \qquad \ldots (B.5)$$

At location X on the value of S_z and accordingly u_{eff} differ from observer to observer and consequently some observers may overtake others. This possibility calls for an observer velocity which is a function of x only. Therefore an element of arbitrariness has to be introduced into the observer velocity calculation.

In the two-dimensional case the growth of S_z with x is determined by differential equation (3.4), which can be solved for a neutrally buoyant situation to give:

$$\left(\frac{S_z}{z_o}\right)_{\rho_z=\rho_a} = \left\{\frac{k}{z_o}\frac{u_*}{u_o}\frac{(1+\alpha)^2}{0.74}(x - x_o)\right\}^{\frac{1}{1+\alpha}} \qquad \ldots (B.6)$$

If we take $x_o = -R_{max}$ and substitute equation (B.6) into equation (B.5), the observer velocity will be given by:

$$\frac{u_o}{\Gamma\frac{1}{1+\alpha}}\left\{k\frac{u_*}{u_o}\frac{(1+\alpha)^2}{0.74}\frac{x + R_{max}}{z_o}\right\}^{\left(\frac{\alpha}{1+\alpha}\right)} \qquad \ldots (B.7)$$

This velocity is definitely too high in a stably stratified situation, since the growth of S_z with x is influenced considerably by vertical density gradients. Therefore, for the observer velocity we put:

$$u_i(x) = C_o \left(\frac{x + R_{max}}{z_o} \right)^{\frac{\alpha}{1+\alpha}} \quad \ldots (B.8)$$

The constant C_o is determined by calculating with the pertinent values of u_o, u_* and ρ_g the value of S_z at the end of a steady-state source of length $L = \sqrt{\pi}\, R_m$, where R_m is the radius of the secondary source when the take-up rate $\pi R^2 Q^*$ is maximum; for the value of Q^* in this calculation the take-up flux at the same time is taken. The observer velocity at $x = \frac{\sqrt{\pi}}{2} R_m$ is then taken to be

$$u_i \left(x - \frac{\sqrt{\pi}}{2} R_m \right) = \frac{u_o}{\Gamma\left(\frac{1}{1+\alpha}\right)} \left(\frac{S_z(x - \frac{\sqrt{\pi}}{2} R_m)}{z_o} \right)^{\alpha} \quad \ldots (B.9)$$

By substituting this expression into equation (B.8) we find:

$$C_o = \frac{u_o}{\Gamma\left(\frac{1}{1+\alpha}\right)} \left[\frac{S_z(x - \frac{\sqrt{\pi}}{2} R_m)}{z_o} \right]^{\alpha} \left\{ \frac{\frac{\sqrt{\pi}}{2} R_m + R_{max}}{z_o} \right\}^{-\frac{\alpha}{1+\alpha}} \quad \ldots (B.10)$$

$$u_i(x) = \frac{u_o}{\Gamma\left(\frac{1}{1+\alpha}\right)} \left[\frac{S_z(x - \frac{\sqrt{\pi}}{2} R_m)}{z_o} \right]^{\alpha} \left\{ \frac{x + R_{max}}{\frac{\sqrt{\pi}}{2} R_m + R_{max}} \right\}^{\frac{\alpha}{1+\alpha}} \quad \ldots (B.11)$$

APPENDIX C

Cloud shape correction for gravitational spreading in the wind direction

In low wind velocities HEGADAS simulations of time-dependent spills show considerable gravitational spreading of high density vapour clouds (e.g. propane) after the initial slumping of the vapour blanket.

Since the HEGADAS model allows for gravitational spreading in the crosswind direction only, the calculated crosswind dimensions are too large and the dimensions in wind direction too small as already indicated in Section 7.

As cloud shape becomes a parameter of increasing importance in more refined hazard assessment methods, we have designed a cloud shape correction routine for the time-dependent HEGADAS computer program. The basic consideration for this correction is that the gravitational spreading velocity should be the same in all directions. The HEGADAS model generates a cloud at a specified point of time consisting of elements with calculated height, length, width and concentration. These elements retain their length while travelling downwind and spreading in the crosswind direction. Leaving height and concentration unchanged as well as the product of length and width of each element, the width is reduced and the length increased in such a way that the amount of spreading in downwind direction of the cloud as a whole equals the spreading in crosswind direction. A subroutine of the HEGADAS time-dependent computer program contains the mathematical formulation of this correction which is briefly outlined below; the notation is consistent with Section 7.

Let L_c be the calculated cloud length and W_c the cloud width at a specified point of time t. As initial cloud width we take the maximum diameter of the gas blanket above the source, $2R_{max}$. We correct cloud width and length now in such a way that the spreading S in downwind direction equals the spreading in crosswind direction. This means, if we define L_c' and w_c' as corrected length and width, that $L_c' = L_c + S$ and $W_c' = 2R_{max} + S$. Conservation of cloud surface area then requires: $L_c' \times W_c' = L_c \times W_c$ or $(L_o^* + S^*) \times (1 + S^*) = L_c^* \times W_c^*$ with $L_c^* = L_c/2R_{max}$, $W_c^* = W_c/2R_{max}$ and $S^* = S/2R_{max}$.

Given L_c^* and W_c^*, equation (13) can be solved for S^*.

$$S^* = -0.5\,(1 + L_c^*) + 0.5\,[(1 + L_c^*)^2 + 4\,L_c^*\,(W_c^* - 1)]^{\frac{1}{2}} \qquad \ldots (C.2)$$

and

$$L'_c/L_c = (L^*_c + S^*)/L^*_c \qquad \ldots (C.3)$$

and

$$W'_c/W_c = (1 + S^*)/W_c^* \qquad \ldots (C.4)$$

Assume now that the uncorrected cloud consists of k elements with length Δx_i and width $D_{eff,i}$ (i=1,k). The cloud shape correction is started at the element where the maximum concentration c_A is found. (If the maximum is found in more than one element, the one located furthest from the source is chosen.) This element remains fixed at its location but its length and width are corrected as follows, in analogy to (C.2) - (C.4):

$$\Delta x'_i/\Delta x_i = (L_c^* + S_i^*)/L_c^* \qquad \ldots (C.5)$$

$$B'_{eff,i}/B_{eff,i} = (1 + S_i^*)/B^*_{eff,i} \qquad \ldots (C.6)$$

with

$$S^*_i = -0.5\,(1+L_c^*) + 0.5\,[(1 + L^*_c)^2 + 4L_c^*\,(B^*_{eff,i}-1)]^{\frac{1}{2}} \qquad \ldots (C.7)$$

where

$$L_c^* = L_c/2R_{max} \qquad \ldots (C.8)$$

and

$$B^*_{eff,i} = B_{eff,i}/B_i \qquad \ldots (C.9)$$

In expression (C.9), B_i is the half-width of element i at the source.

Again, these correction formulae satisfy the essential condition of conservation of element surface area:

$$\Delta x'_i \times B'_{eff,i} = \Delta x_i \times B_{eff,i}$$

The shape correction of the elements upwind and downwind of the first one are performed in an identical way.

Correction (B6) is applied to both the middle part and the Gaussian flanks of the crosswind concentration profile:

$$b'_i/b_i \; S'_{yi}/S_{yi} = (1 + S_i^*)/B^*_{eff,i}$$

No correction is applied when $b_i = 0$

After the correction gravitational slumping, dispersion in the wind direction is taken into account as described in Section 7.

APPENDIX D

Laboratory experiemnts on heat and mass transfer into a cold nitrogen gas flow

Laboratory experiments were performed to test the aspects of heat transfer, water vapour transfer and convective entrainment in the model. Results have been presented in the main text. The experimental setup is summarised here; more details have been given by Colenbrander and Puttock (1984).

Three series of experiments were performed. In series 1 a steady stream of liquid nitrogen (-196°C) was released into a 1m wide and 0.2m deep tray filled with water up to about 3cm below the brim. The nitrogen, floating on the water surface, evaporated and the cold, dense vapour entered a perspex box, the flow being homogeneously distributed over the width of the box (see Figure 11). The box contained a water layer 0.2m deep, over the surface of which the vapour was flowing. The nitrogen left the box through an opening over its entire width. The opening was provided with a flow restriction consisting of vertical bars with a triangualar cross-section. The length and width of the box were equal (1m), and the height was 0.6m. On top a lid was placed to prevent air currents in the room from affecting the flow in the box. Holes in the lid allowed air to flow in and out freely.

In series 2 the water surface in the evaporation tray was covered with a copper plate from which the nitrogen was evaporated. Hot water was circulated through the tray below the plate to provide the heat of vaporisation.

In series 3 this copper plate was used again, but in addition the water surface in the box was covered with an oil film. This was done to prevent water vapour transfer from the water surface into the nitrogen vapour stream.

At locations A, B and C (0.25, 0.50 and 0.75m from the box entrance) temperatures and concentrations in the vapour stream were measured. A mass spectrometer was used to measure the concentrations of nitrogen, oxygen and water, from which were calculated air entrainment and water (vapour) pick-up into the nitrogen vapour stream.

The water temperature in the box was measured, as well as a vertical temperature profile in the vapour stream at location B, which indicated the vapour layer thickness. In all test runs the temperature was measured simultaneously at all locations. But the concentrations could only be measured at one fixed location during a run. Repeat runs were performed so that concentration measurements could be obtained at a number of locations.

APPENDIX E

Summary of HEGADAS equations

For clarity the complete set of equations solved by HEGADAS is summarised in this appendix.

The HEGADAS formulation of dispersion in vertical direction is given by:

$$\frac{d}{dx}\left[u_{eff}\ B_{eff}\ H_{eff}/V_m\right] = Q_*\ B_{eff} \tag{E.1}$$

with,

$$Q_* = \left[ku_T(1+\alpha)/(V_{ma}\Phi(Ri_T)) + Q_{wv}\right] \tag{E.2}$$

In this expression

$$u_T = u_*^2 + (0.2\ w_*)^2 \tag{E.3}$$

$$w_* = \left[\frac{g\ Q_H\ H_{eff}}{T_m \rho_m\ C_{pm}}\right]^{1/3} \tag{E.4}$$

$$Ri_T = g'\ \frac{H_{eff}}{u_T^2} \tag{E.5}$$

with $$g' = g[\rho_m(c-c_A) - \rho_a(z - H_{eff})]/\rho_a(z = 0) \tag{E.6}$$

The temperature T_m and density $\rho_m(c-c_A)$ of the gas/air mixture as well as the specific molar volume V_m are computed in the thermodynamic subroutine THERMO.

Expressions for u_{eff}, B_{eff} and H_{eff} read:

$$u_{eff} = u_o \left(\frac{S_z}{z_o}\right)^{\alpha} \frac{1}{\Gamma\left(\frac{1}{1+\alpha}\right)} \qquad (E.7)$$

$$B_{eff} = b + \frac{\sqrt{\pi}}{2} S_y \qquad (E.8)$$

and,

$$H_{eff} = \frac{\Gamma\left(\frac{1}{1+\alpha}\right)}{1+\alpha} S_z \qquad (E.9)$$

Hence Equation (E.1) may also be written as:

$$\frac{d}{dx}\left[(b + \frac{\pi}{2} S_y) \left(\frac{S_z}{z_o}\right)^{1+\alpha} / V_m \right] = \frac{1+\alpha}{u_o\ z_o} (b + \frac{\pi}{2} S_y)\ Q_* \qquad (E.10)$$

Above the source S_y is taken to be zero and b as well as c (and V_m) are taken to be constant and hence Equation (E.10) reduces to

$$\frac{d}{dx}\left[\left(\frac{S_z}{z_o}\right)^{1+\alpha} \right] = \frac{1+\alpha}{u_o\ z_o} V_m\ Q_* \qquad (E.11)$$

Since heat transfer from the earth's surface and water vapour pick-up are neglected above the source ($D = 0$ and $y_{w3} = 0$), Equation (E.11) is the only differential equation to be solved above the source. Q_* then reduces to:

$$Q_* = [k u_* (1+\alpha)/(V_o \Phi(Ri_*))] \qquad (E.12)$$

If the atmosphere cannot take up directly by diffusion the gas flux emitted by the source, a 100% gas blanket is formed in the model

formulation. The dimensions of the gas blanket are determined iteratively in such a way that the molar flow rate of gas transported by the wind equals the emission rate. This calculation is done along the lines set out by Colenbrander (1980, Section 2.3), who also discusses the case of no formation of a gas blanket. This occurs if the atmospheric take-up is greater than the emission rate. Then the ground-level gas concentration above the source is less than 100%, while the source dimensions are determined by the source specification. The constant value of c above the source is again determined iteratively so as to satisfy continuity of gas molar flow rate.

Downwind of the source, at distances where the middle part of the concentration profile b has not yet disappeared, the entrainment relation (E.11) is solved together with four additional differential equations.

The first of these four is an equation describing heat transfer:

$$\frac{d}{dx} [\ D\ u_{eff}\ B_{eff}\ H_{eff}/V_m\ ]\ -\ Q_H\ B_{eff} \qquad (E.13)$$

or

$$\frac{d}{dx}\left[D(b + \frac{\pi}{2} S_y) \left(\frac{S_z}{z_o}\right)^{1+\alpha} /V_m \right] - \frac{1+\alpha}{u_o\ z_o} (b + \frac{\sqrt{\pi}}{2} S_y)\ Q_H \qquad (E.14)$$

The second equation describes the pick-up of water vapour:

$$\frac{d}{dx}\ [y_{w3}\ u_{eff}\ B_{eff}\ H_{eff}/V_m\ ]\ -\ Q_{wv}\ B_{eff} \qquad (E.15)$$

or

$$\frac{d}{dx}\left[y_{w3}(b + \frac{\pi}{2} S_y) \left(\frac{S_z}{z_o}\right)^{1+\alpha} /V_m \right] - \frac{1+\alpha}{u_o\ z_o} (b + \frac{\sqrt{\pi}}{2} S_y)\ Q_{wv} \qquad (E.16)$$

The third additional equation deals with the lateral gravitational spreading of the plume:

$$\frac{dB_{eff}}{dt} = C_E \sqrt{g\left[1 - \frac{\rho_a(z=0)}{\rho(\omega)}\right]H_{eff}} \qquad (E.17)$$

or

$$\frac{d}{dx}\left(b + \frac{\sqrt{\pi}}{2} S_y\right) = C \sqrt{1 - \frac{\rho_a(z=0)}{\rho(\omega)}} \left(\frac{S_z}{z_o}\right)^{\frac{1}{2}-\alpha} \qquad (E.18)$$

where we use 1.15 for the spreading constant C_E and

$$C = C_E \left(\frac{gz_o}{u_o^2}\right)^{\frac{1}{2}} \left\{\Gamma\left(\frac{1}{1+\alpha}\right)\right\}^{3/2} (1+\alpha)^{-\frac{1}{2}} \qquad (E.19)$$

Finally an equation is added to describe the crosswind atmospheric dispersion:

$$S_y \frac{dS_y}{dx} = \frac{4\beta}{\pi}\left(b + \frac{\sqrt{\pi}}{2} S_y\right)^2 \left\{\frac{\delta \sqrt{\pi}/2}{b + \frac{\sqrt{\pi}}{2} S_y}\right\}^{1/\beta} \qquad (E.20)$$

where β and δ are constants in a relation, determining the crosswind spreading of a plume, emitted by a point source.

To close the set of equations, c is determined by dividing the molar flow rate of emitted gas by the total flow rate $u_{eff}\ B_{eff}\ H_{eff}/V_m$ in the plume. Given y_{w_8} c, D and y_{w3}, the plume temperature T_m, density $\rho(c)$ and specific molar volume V_m are calculated in the subroutine THERMO. Hence the 7 unknowns S_z, S_y, b, D, y_{w3}, c and V_m are determined by solving the set of 5 coupled ordinary differential Equations (E.10), (E.14), (E.16), (E.18) and (E.20), together with the integral molar mass and enthalpy balances (THERMO).

Downwind of the point $x = x_t$ where b becomes zero, gravitational spreading is neglected and hence (E.18) is dropped from the set of equations. Since the crosswind concentration profile is completely Gaussian for $x > x_t$, Equation (E.20) can be solved, giving

$$S_y = 2\,\delta(x + x_v)^{\beta} \tag{E.21}$$

where x_v is determined from the expression

$$S_y(x_t) = 2\,\delta(x_t + x_v)^{\beta} \tag{E.22}$$

For $x > x_t$ Equations (E.10), (E.14) and (E.16) reduce to

$$\frac{d}{dx}\left[\left(\frac{S_z}{z_o}\right)^{1+\alpha} \sqrt{V_m}\right] = \frac{1+\alpha}{u_o\, z_o} Q_e \tag{E.23}$$

$$\frac{d}{dx}\left[D\left(\frac{S_z}{z_o}\right)^{1+\alpha} \sqrt{V_m}\right] = \frac{1+\alpha}{u_o\, z_o} Q_H \tag{E.24}$$

and

$$\frac{d}{dx}\left[y_{w3}\left(\frac{S_z}{z_o}\right)^{1+\alpha} \sqrt{V_m}\right] = \frac{1+\alpha}{u_o\, z_o} Q_{wv} \tag{E.25}$$

Table A1

Some useful physical constants for hydrocarbons, water and air

Constant	Methane	Ethane	Propane	n-Butane	Ethylene	Propylene	Nitrogen	Air	Water vapour
Molecular weight M_g	16.04	30.07	44.0	58.13	28.05	42.08	28.016	28.964	18.016
Boiling point T_g', ^oC	-161.5	-88.6	-42.07	-0.5	-103.7	-47.5	-195.8	-	-
Latent heat of vaporisation at boiling point h^*_{gv} (J/mole)	8200	14 700	18 800	22 400	13 500	18 400	5578	-	45 000 at 0^oC
(vapour)	34.4	48.0	68	96.6	39	60.4	29.3	29.1	Heat of fusion H^*_{wf} : 6010
(liquid)									33
(solid)									(c^*_{pwl}) 75.5
									(c^*_{pwi}) 37.9[+]
Liquid density at b.p.	424	548	580	603	570	591	807	-	-
Thermal diffusivity/ $(\text{temperature})^2$, $m^2/s\ K^2$	2.6×10^{-10}	0.95×10^{-10}	0.61×10^{-10}	0.41×10^{-10}	1.20×10^{-10}		2.7×10^{-10}	2.5×10^{-10}	-
Kinematic viscosity/ $(\text{temperature})^2$, $m^2/s\ K^2$	1.92×10^{-10}	0.85×10^{-10}	0.50×10^{-10}	0.34×10^{-10}	1.00×10^{-10}	0.54×10^{-10}	2.0×10^{-10}	1.8×10^{-10}	-
Upper flammable limit, %	15.0	12.8	9.4	8.4	30	11	-	-	-
Lower flammable limit, %	5.0	2.9	2.1	1.8	2.7	2.0	-	-	-

[+] A better value for the mean between 0^oC and the boiling point of the gas T_g' is: $c^*_{pwi} = 37.0 + 0.066\ T_g'$ with T_g' in degrees C.

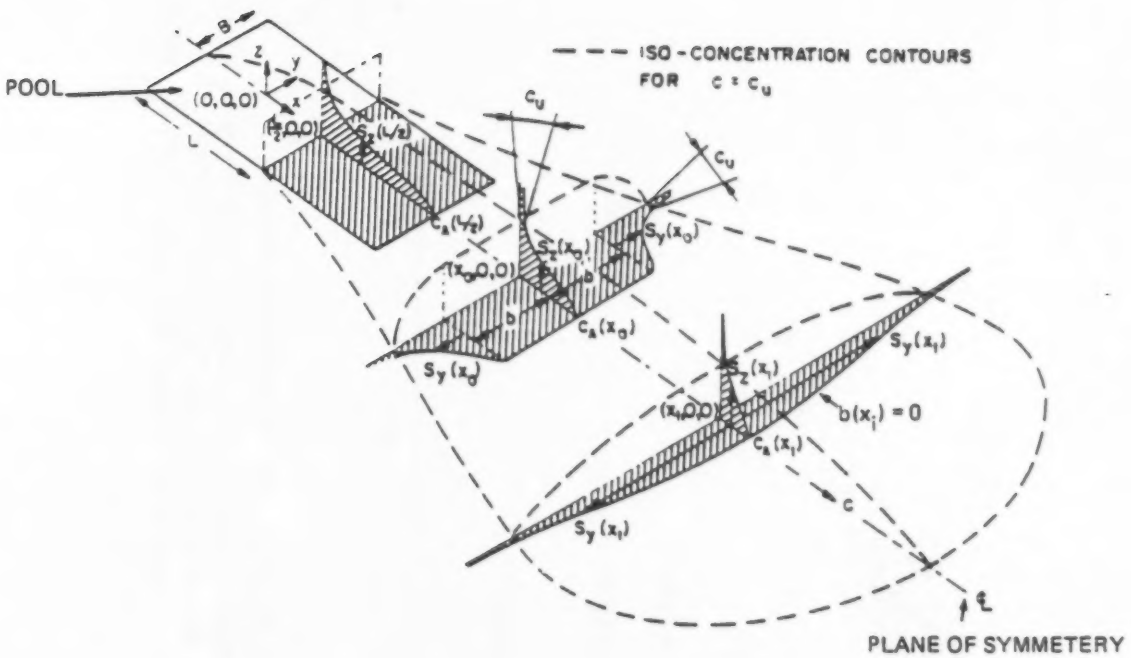

FIG. 1 — The similarity profiles for the concentration and iso-concentration contours in the planes $y = 0$, $z = 0$, $x = L/2$, $x = x_o$ and $x = x_1$

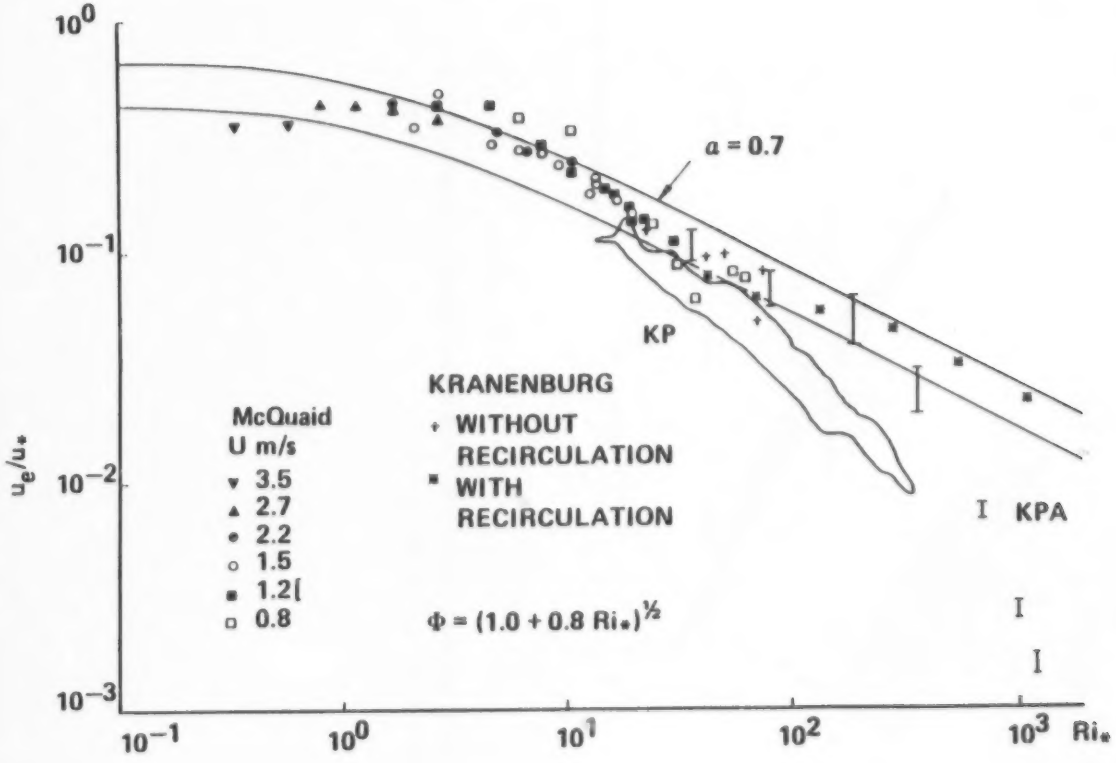

FIG. 2 — Dimensionless entrainment velocity u_e/u_* as a function of the bulk Richardson number Ri_*. The error bars indicate the results of the KPA experiments, corrected for side-wall drag ($H/W \rightarrow 0$). The KP data are continuously distributed within the cloud outlined in this Figure; these data are for $H/W \leqslant 0.6$. The solid lines represent our fit to the Kranenburg and McQuaid data: $u_e/u_* = 0.41\ (1+a)/\Phi(Ri_*)$

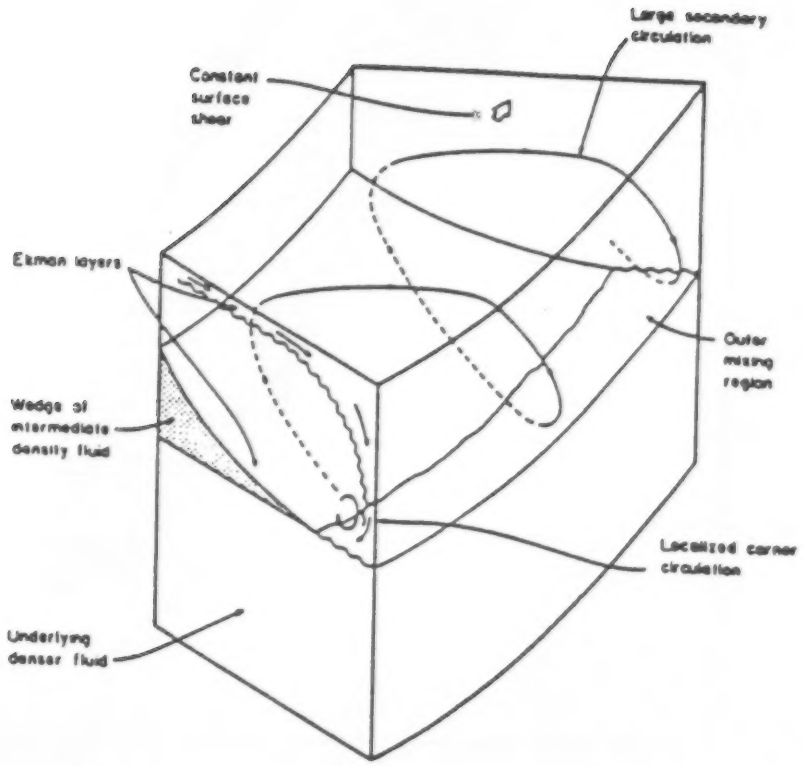

FIG. 3 . Conceptual flow model for moderate and high Richardson numbers ($Ri_* > 100$), showing outer interfacial mixing region, wedge of intermediate density fluid, secondary flow, and localized corner circulation.

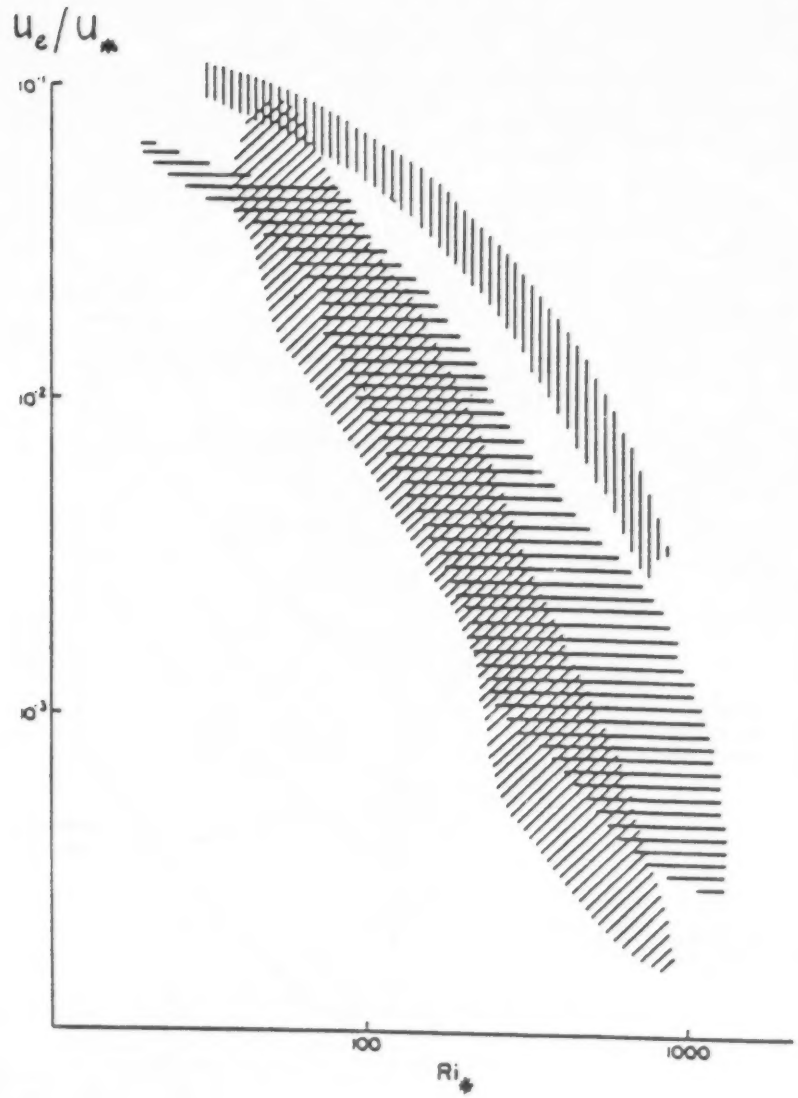

FIG. 4. Measured entrainment rates of various investigators. The bands shown are envelopes of reported experimental data for various parametric variations, where the greatest variation was in the mean radius and values of H/W: |||| is Kantha, Phillips, and Azad, $R_m = 65$ cm, $H/W = 0.25$; ≡ is Deardorff and Willis, $R_m = 50$ cm, $H/W = 0.38$–1.5; ///// is Scranton and Lindberg, $R_m = 53$ cm, $H/W = 0.25$–0.37. The data of Kato and Phillips fall in the band of data common to Deardorff and Willis and Scranton and Lindberg, and is not shown (for clarity).

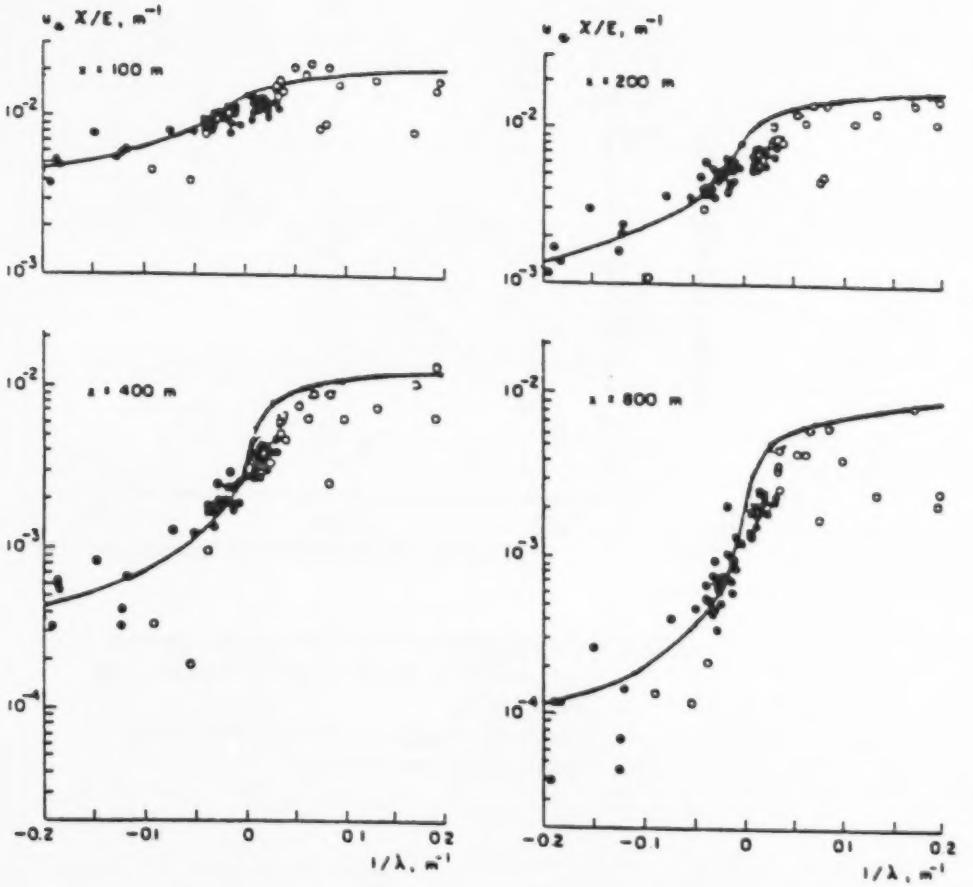

FIG 5 MEASURED (POINTS) AND PREDICTED (CURVE) CONCENTRATIONS 100, 200, 400 AND 800 m DOWNWIND OF THE SOURCE IN THE PRAIRIE GRASS EXPERIMENTS

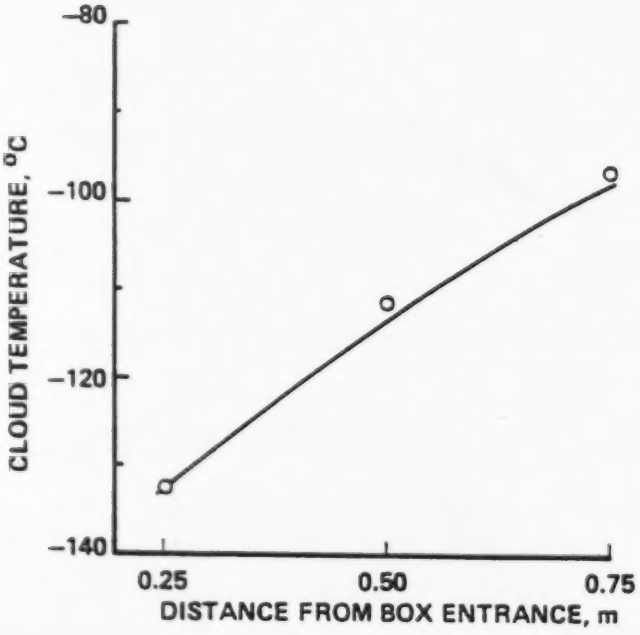

FIG. 6 – Temperature as a function of distance from box entrance, measured and calculated with HEGADAS;
Series 3 : Evaporation from copper plate, oil film on water surface.

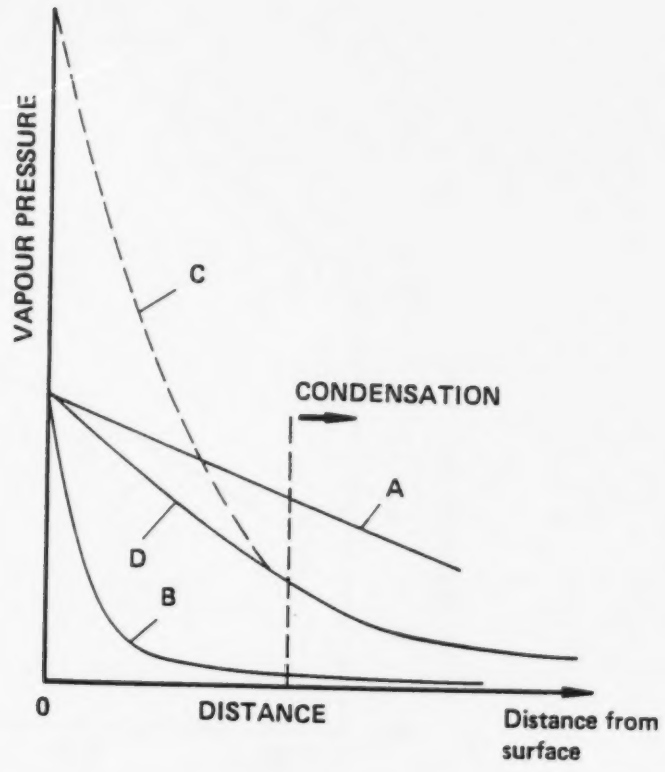

FIG. 7 – Vapour pressure profiles in the immediate vicinity of a vaporising surface (after Rosner, 1967)

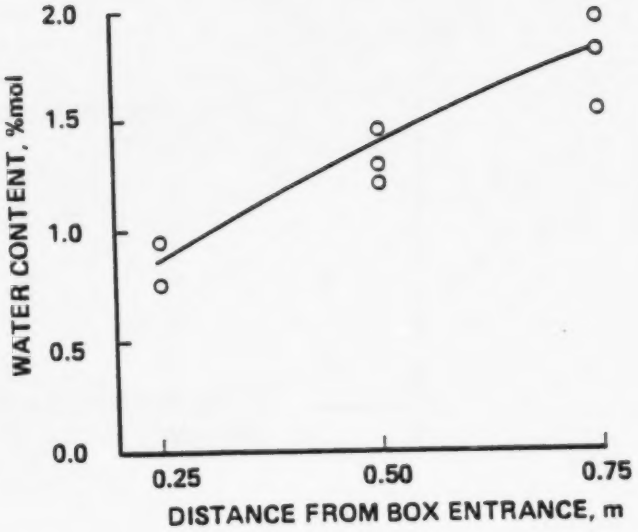

FIG. 8 — Water concentration as a function of distance; experimental data points; curve calculated with HEGADAS
Series 2: Evaporation from copper plate.

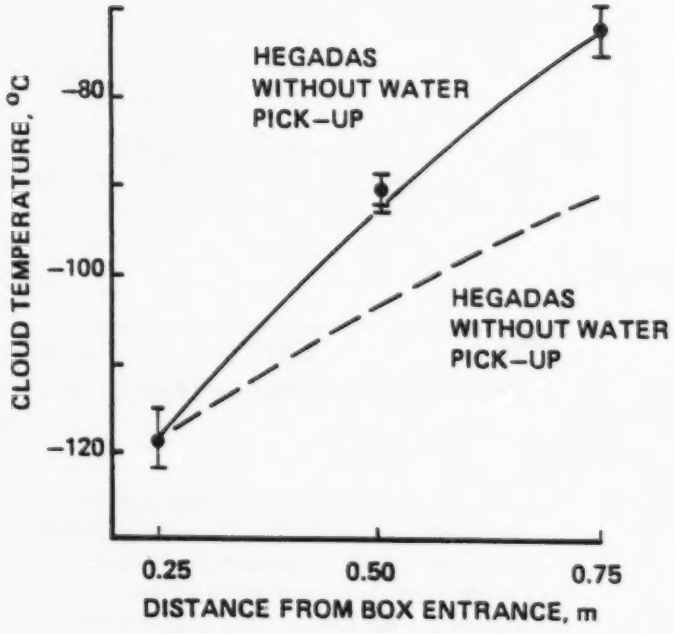

FIG. 9 – Temperature as a function of distance; the bars represent the experimental data, the curve results from a HEGADAS calculation.
Series 2: Evaporation from copper plate

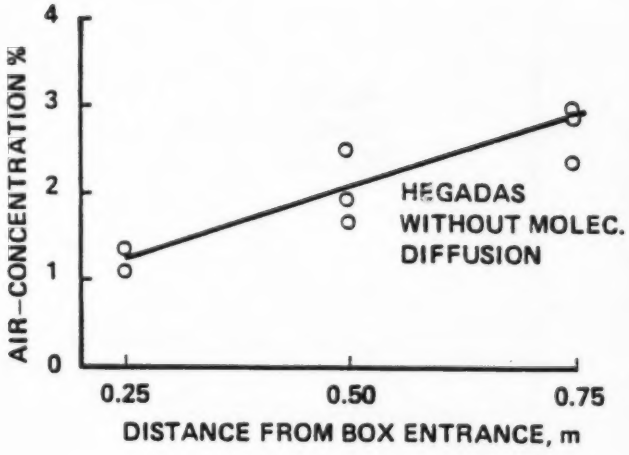

FIG. 10 – Air concentration (molar percentage of air in air/nitrogen mixture) as a function of distance; experimental data points and curves, calculated with HEGADAS
Series 2: Evaporation from copper plate.

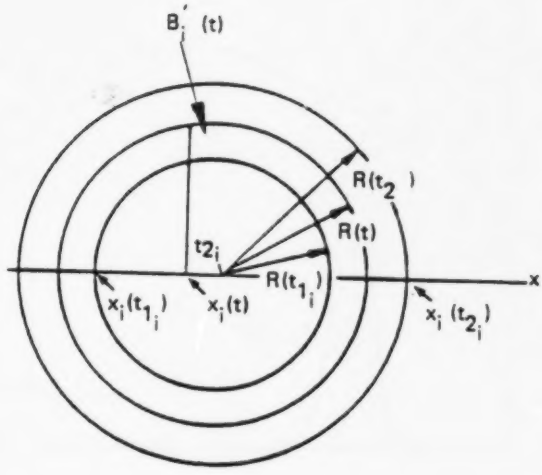

FIG. 11 – Parameters associated with observer "i"

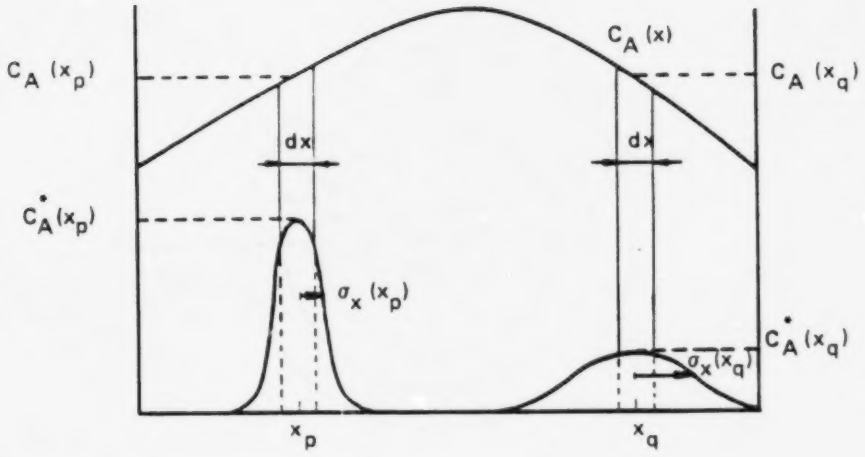

FIG. 12 – Correction of the concentration distribution $C_A(x)$ for dispersion in the x–direction

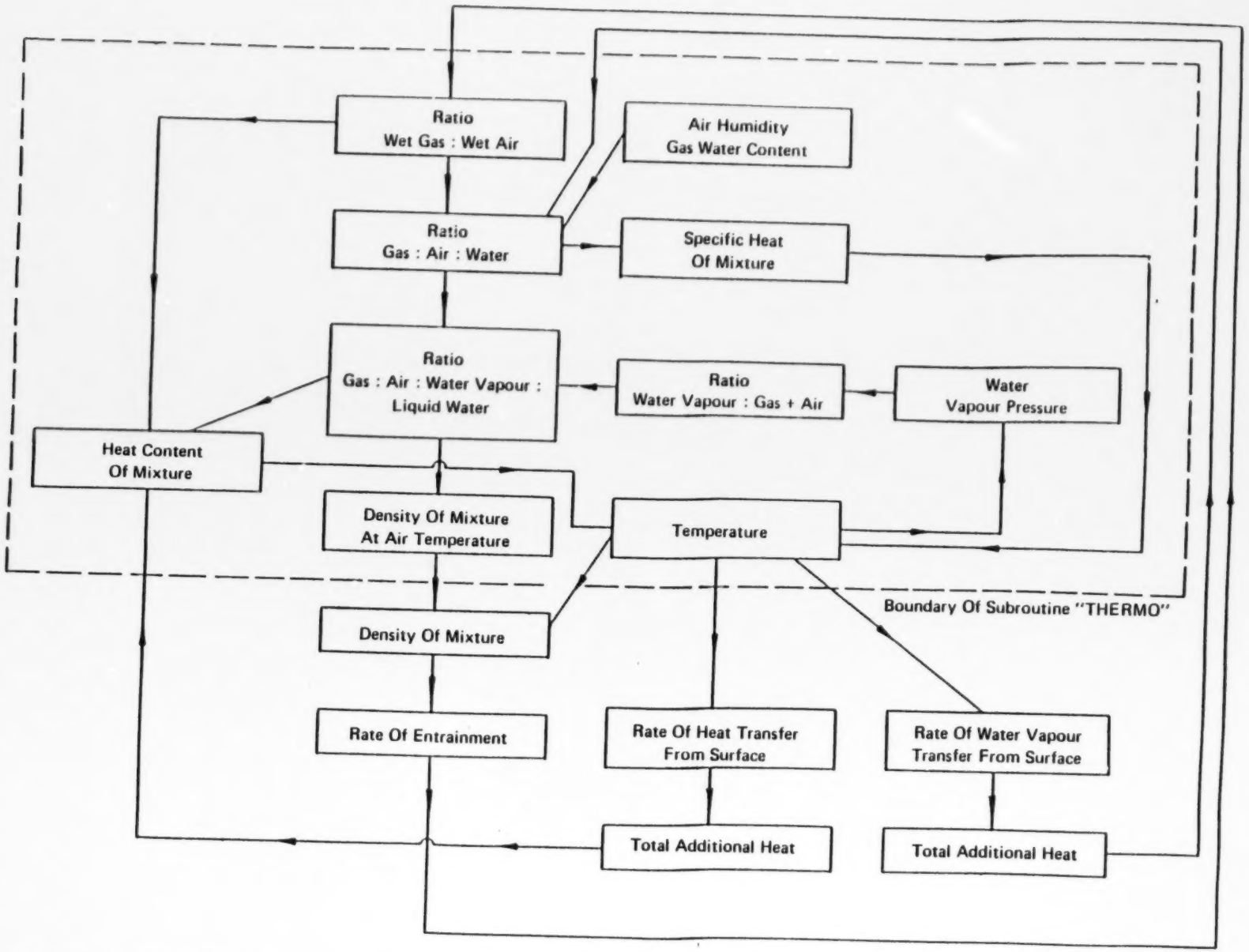

FIG. 13 – The interdependence of the various thermodynamic quantities, which determines the sequence of calculation in the thermodynamic subroutine of HEGADAS. Simplifying assumptions are perfect gas behaviour and quantities such as specific heat independent of temperature